Eagleworks Laboratories

WARP FIELD PHYSICS

Dr. Harold "Sonny" White
NASA JSC

Picture courtesy of NASA,
http://www.nasa.gov/centers/glenn/technology/warp/warpstat.html

Hyper-fast interstellar travel…

- Is there a way within the framework of physics such that one could cross any given cosmic distance in an arbitrarily short period of time, while never locally breaking the speed of light (11th commandment)?

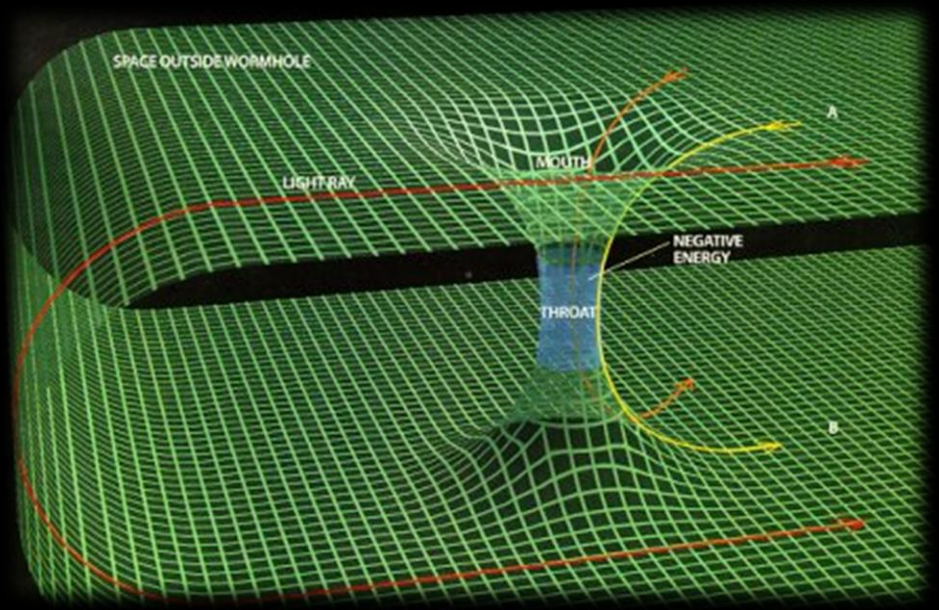

WORMHOLES (shortcuts)

SPACEWARPS (inflation)

Images courtesy NASA

Inflation: Alcubierre Metric[1]

Warp Metric:

$$ds^2 = -dt^2 + (dx - v_s f(r_s)dt)^2 + dy^2 + dz^2$$

Apparent speed

Shaping Function:

Shell thickness parameter

Shell size parameter

$$f(r_s) = \frac{\tanh(\sigma(r_s + R)) - \tanh(\sigma(r_s - R))}{2\tanh(\sigma R)}$$

York Time:

$$\theta = v_s \frac{x_s}{r_s} \frac{df(r_s)}{dr_s}$$

York Time is measure of expansion/contraction of space

Energy Density:

$$\frac{1}{8\pi} G^{00} = -\frac{1}{8\pi} \frac{v_s^2 (y^2 + z^2)}{4 r_s^2} \left(\frac{df(r_s)}{dr_s} \right)^2$$

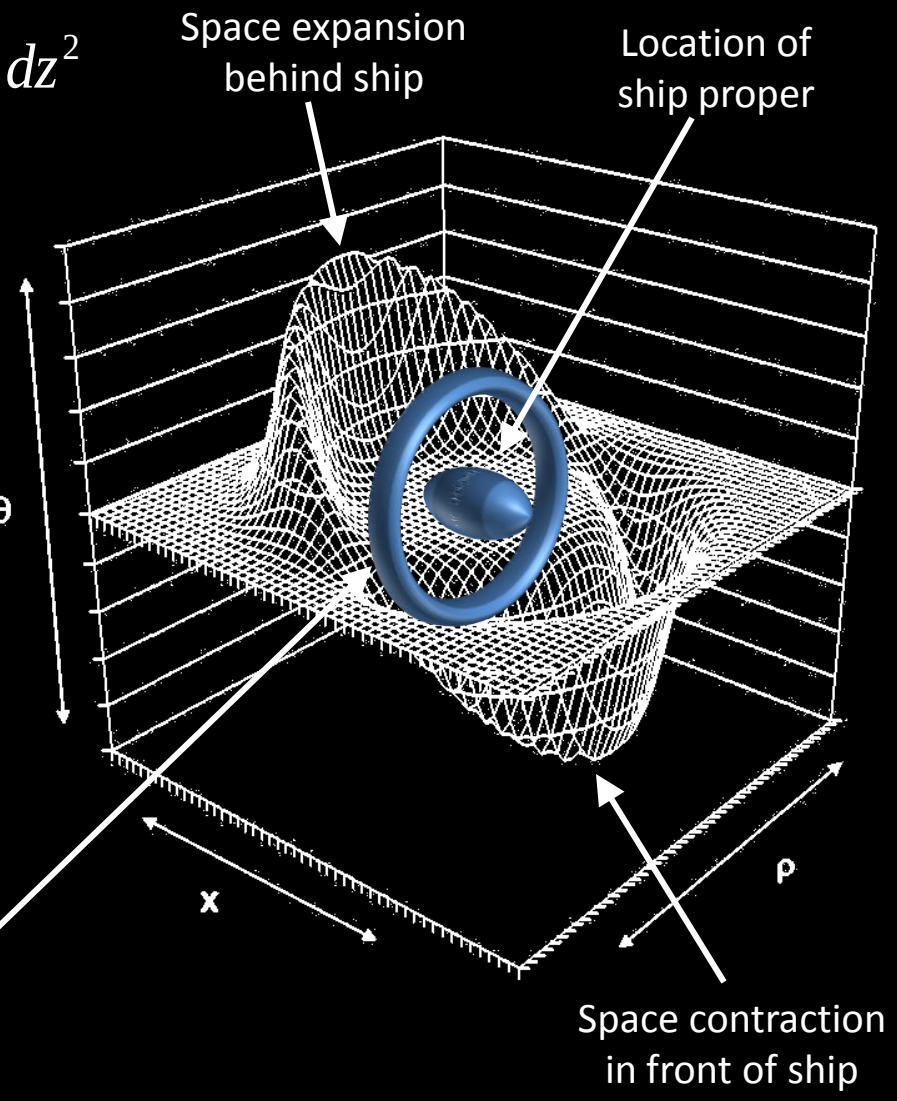

1. Alcubierre, M., "The warp drive: hyper-fast travel within general relativity," Class. Quant. Grav. 11, L73-L77 (1994).

Bubble Topology Optimization

York Time magnitude decreases

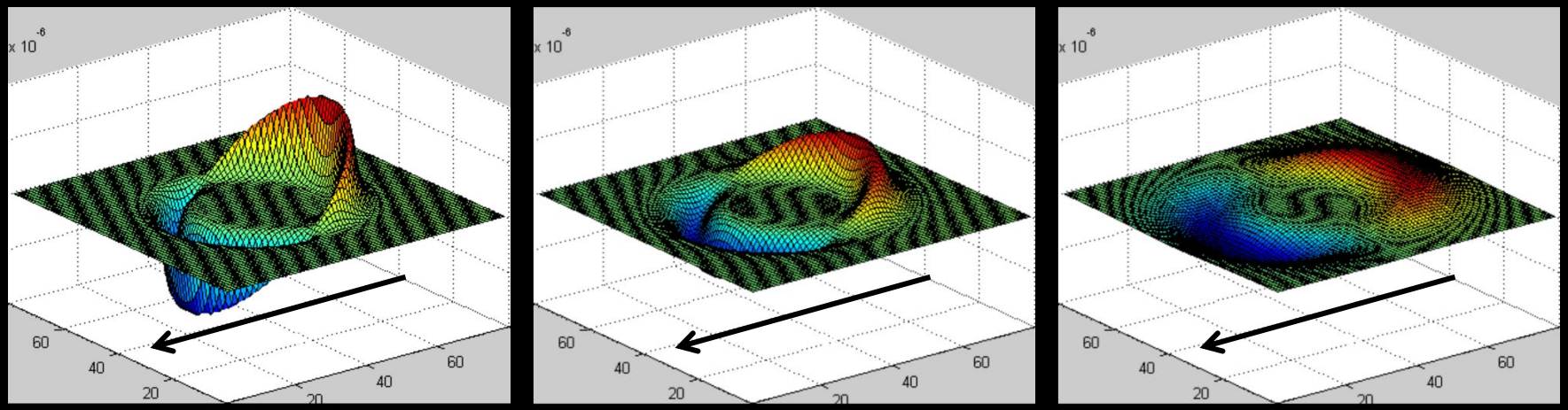

"bubble" thickness decreases

Energy density magnitude decreases

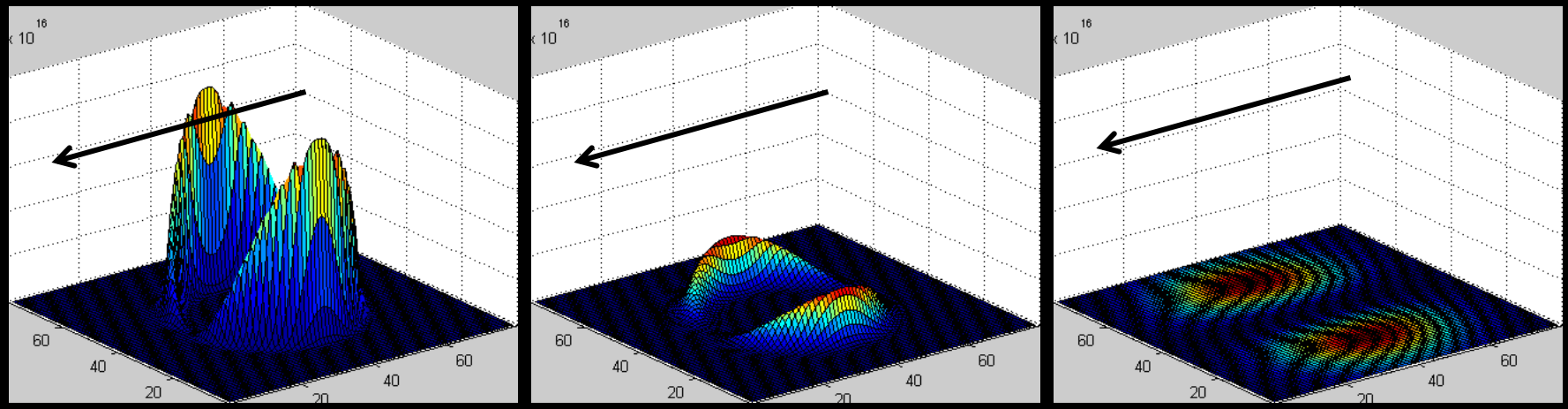

"bubble" thickness decreases

Surface plots of York Time & T^{00}, <v>=10c, 10 meter diameter volume, variable warp "bubble" thickness

Bubble Oscillation Optimization

$$ds^2 = -c^2dt^2 + \frac{a^2(t)}{e^{2kU}}dX^2 + dU^2$$

$$\frac{dX}{dt} = \frac{ce^{kU}}{a(t)}\sqrt{1 - \frac{dU^2}{c^2dt^2}}$$

$$\frac{dU}{dt} \Rightarrow 1, U = 0 \quad \therefore \frac{dX}{dt} \Rightarrow 0$$

$$\gamma \approx e^U \quad \phi \approx U \quad \frac{d\phi}{dt} \approx \frac{dU}{dt}$$

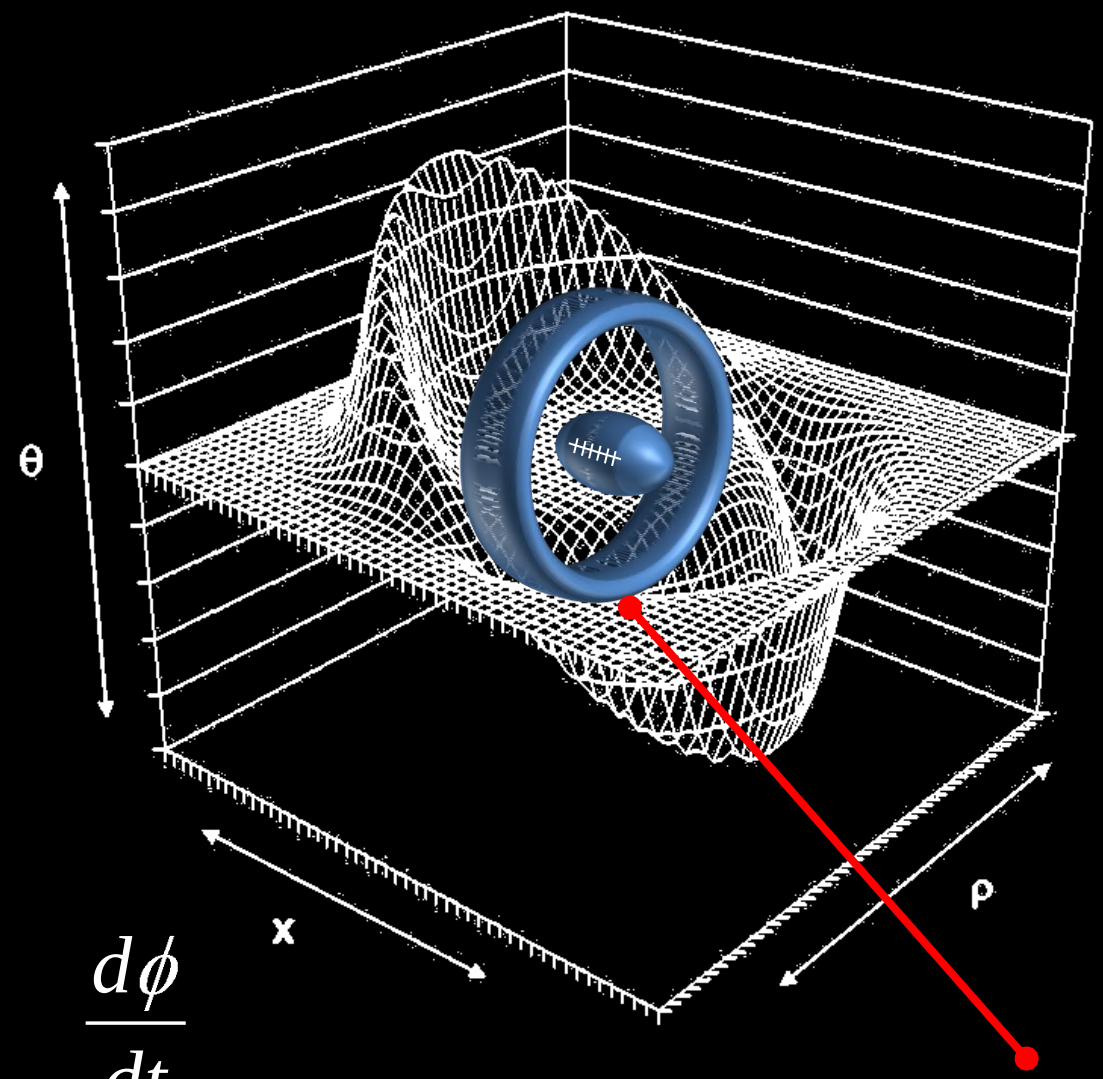

$$\frac{d\phi}{dt}$$

Oscillate the bubble intensity

Images courtesy NASA

Exotic Mass Warp Requirements, 10m diameter, $v_{apparent}$=10c

THINNER BUBBLE/RING ← Shell Thickness Fraction (2*R/S) → THICKER BUBBLE/RING

no flat space left in bubble

1.00E-05 | 1.00E-04 | 1.00E-03 | 1.00E-02 | 1.00E-01 | 1.00E+00

Total exotic mass (kg)

1.00E+28 | 1.00E+26 | 1.00E+24 | 1.00E+22 | 1.00E+20 | 1.00E+18 | 1.00E+16 | 1.00E+14 | 1.00E+12 | 1.00E+10 | 1.00E+08 | 1.00E+06 | 1.00E+04 | 1.00E+02 | 1.00E+00

FASTER HYPERSPACE VELOCITY/OSCILLATIONS

graph by Dr. Harold "Sonny" White

Chung-Freese null geodesics

$$\frac{dX}{dt} = \frac{ce^{kU}}{a(t)}\sqrt{1-\frac{dU^2}{c^2dt^2}}$$

Jupiter 1.9×10^{27}

Earth 6.0×10^{24}

Moon 7.4×10^{22}

4Vesta 2.6×10^{20}

Bulk Velocity, dU/dt
- dU/dt=0c
- dU/dt=0.9c
- dU/dt=0.999c
- dU/dt=0.99999c
- dU/dt=0.9999999c
- dU/dt=0.999999999c

Nimitz carrier 9.1×10^{7}

ISS 4.0×10^{5}

Dragon/

Voyager

Energy Density Topology Approximations

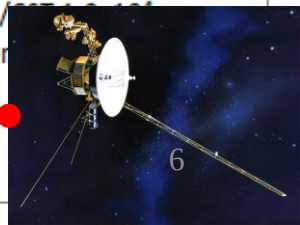

Warp Field Interferometer

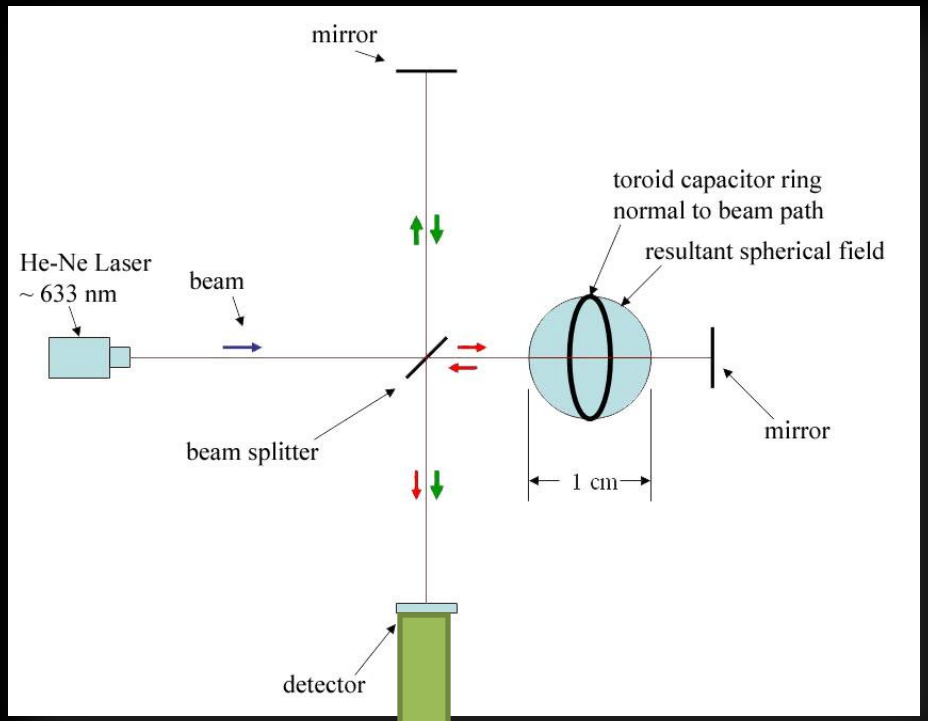

- Warp Field Interferometer developed after putting metric into canonical form[1]:

$$ds^2 = (v_s{}^2 f(r_s)^2 - 1)\left\{dt - \frac{v_s f(r_s)}{v_s{}^2 f(r_s)^2 - 1}dx\right\}^2 - dx^2 + dy^2 + dz^2$$

- Generate microscopic warp bubble that perturbs optical index by 1 part in 10,000,000
- Induce relative phase shift between split beams that should be detectable.

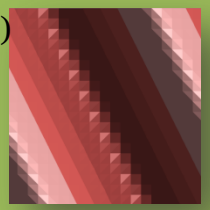

Numerical simulation of fringe at detector with device off

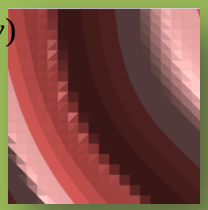

Numerical simulation of fringe at detector with device on

2D Analytic Signal processing

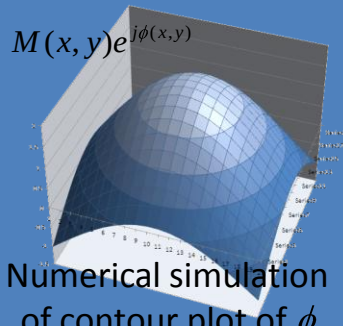

Numerical simulation of contour plot of ϕ for warp field

1. White, H., "A Discussion on space-time metric engineering," Gen. Rel. Grav. 35, 2025-2033 (2003).

Warp Bubble Detection Attempts Using Interferometry

- **Goal is to use interferometer to detect and measure effect of warp bubble on optical path length through the measurement of associated interference fringe shifts.**
- The EWL has attempted to mitigate the effect of vibrations & air currents
  - Using a vibration-isolated optical table
  - Using a vibration-isolated room
  - Using an optical hood
  - Using signal processing to increase signal to noise ratio
  - Collecting statistical data to increase signal to noise ratio

Eagleworks Optics Laboratory

Time of Flight
Experiment

Warp field
Interferometer

Interferometer and Test-article Setup

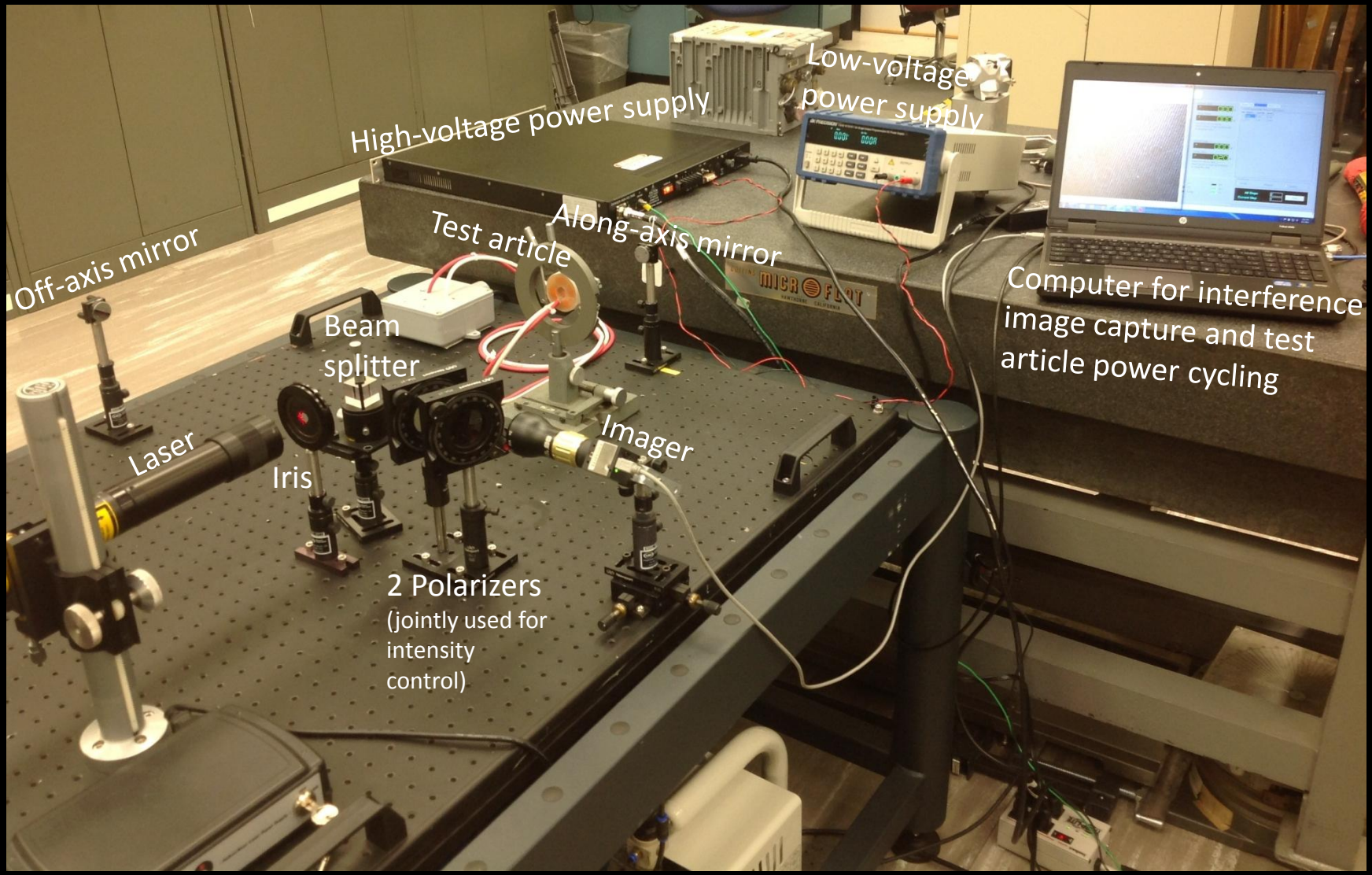

Isolated Lab

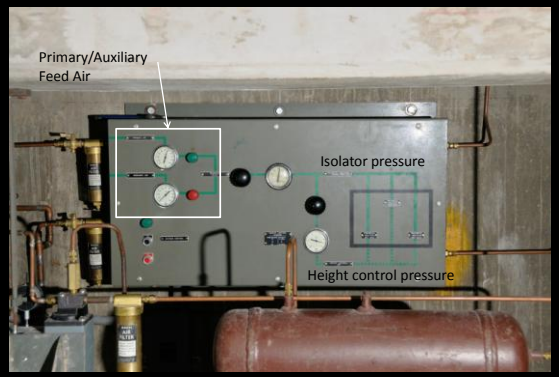

SINGLE PATCH

INTERFEROMETER MODAL ANALYSIS, ANALYTIC SIGNAL VARIATION

Interferometer Modal Analysis: Synthetic Data

- A set of 1000 synthetic interferogram fringe patterns were generated as JPEG image frames
  - Set contained repeating sequence of 10 frames with sinusoidal shifting in time with a shifting amplitude of 1/10 of a spatial radian*.
  - No noise added to the shifting (i.e. unwanted vibrations not included)
  - **Gray scale intensity sampled at upper left pixel** and a Discrete Fourier Transform (DFT) calculated for the sample train.
  - Very strong peak observed at 1/5 Nyquist frequency as expected, and of course, no noise spectrum.

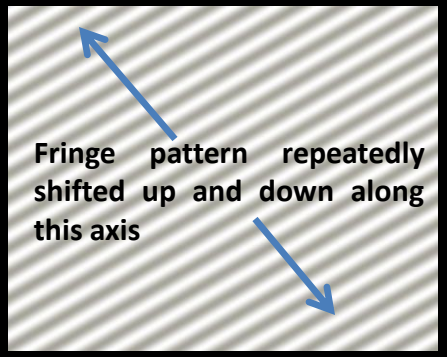

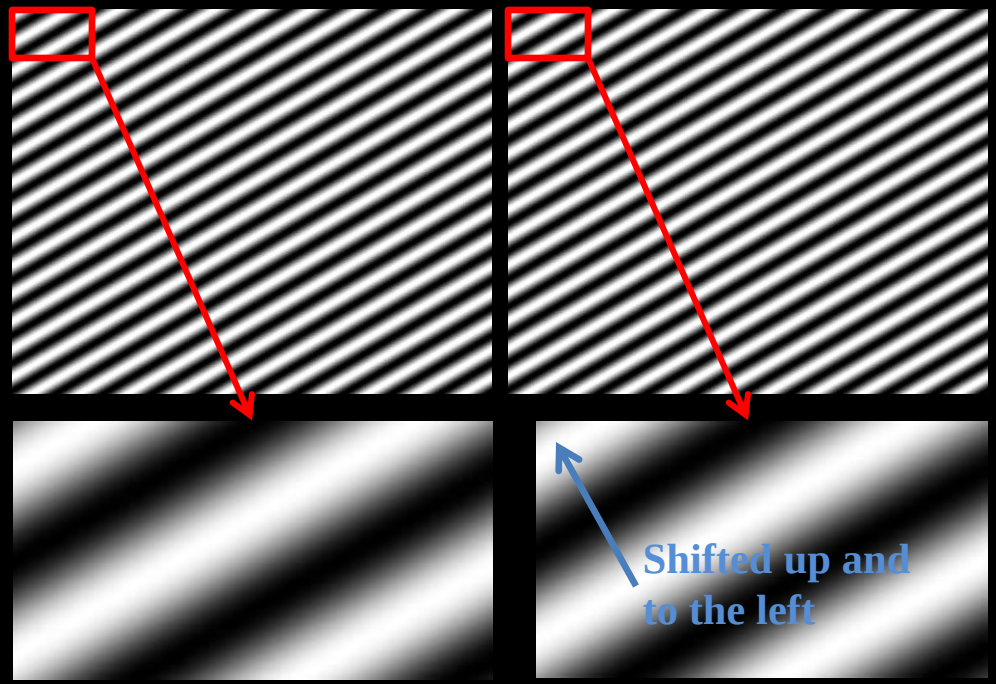

2 fringe patterns out of set of 1000, showing maximum shift amplitude (In this case, the fringe pattern on the right is shifted about 1 radian up and to the left compared to the fringe pattern on the left.)

DFT Magnitude Spectrum

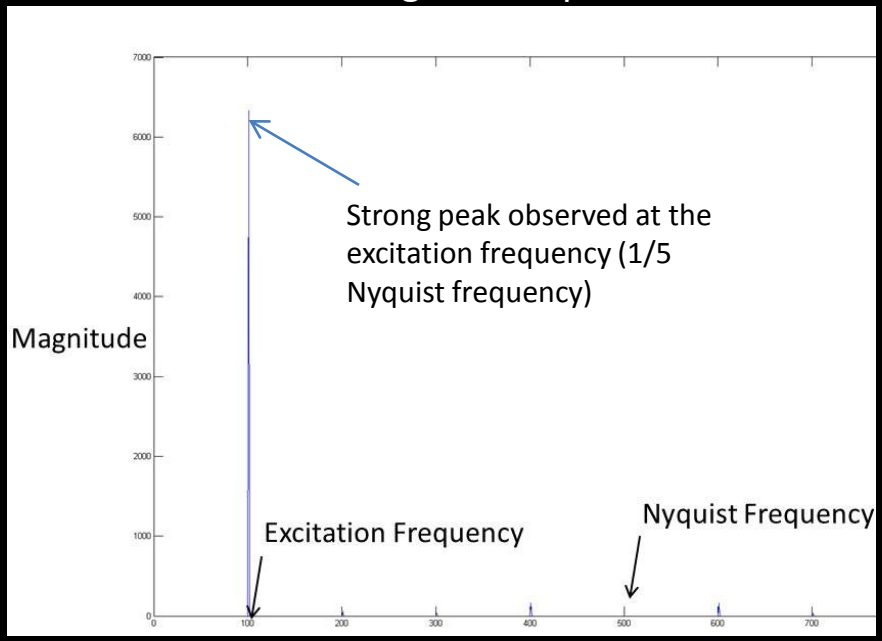

Conclusion: Small, repetitive shifts in fringe lines can be easily detected with a temporal DFT approach.

Modal Analysis: Analytic Signal Variation, Single Patch

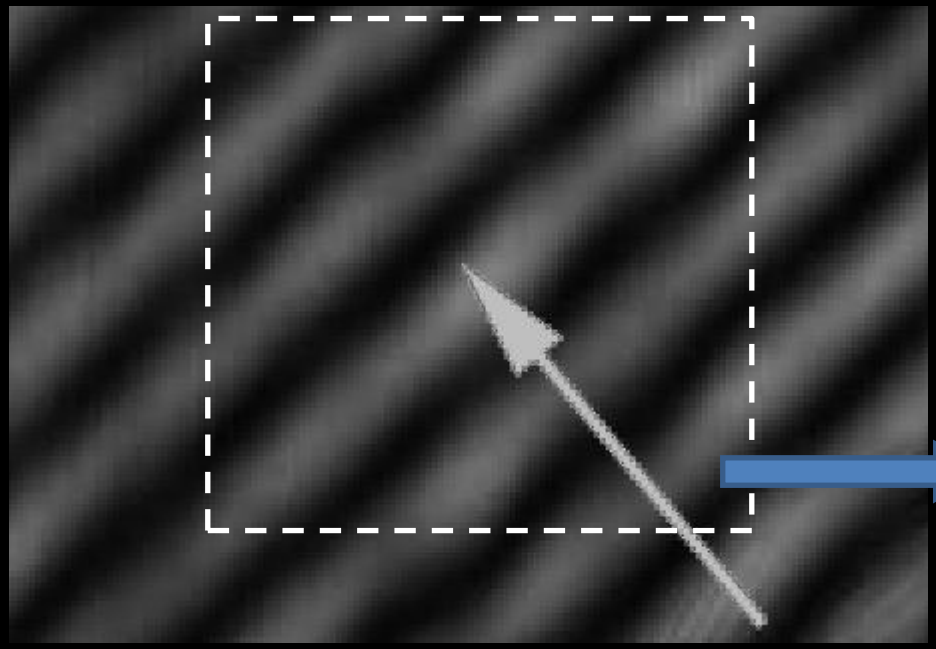

Calculate DFT of this 128x128 region centered at arrow tip.

2D DFT of the dashed region

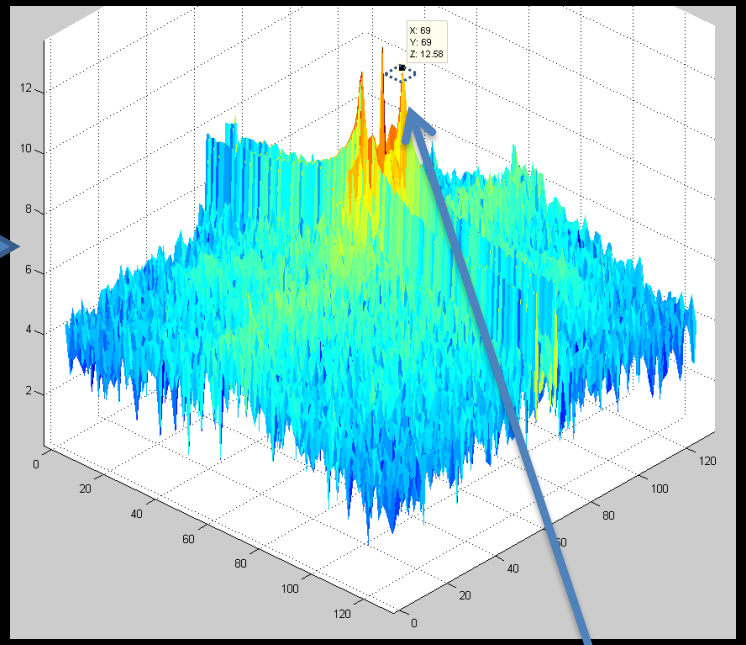

The result is an array of complex values, called the analytic signal. Use the complex value at the center and calculate the "phase". Repeat for all of the captured frames and store the representative phase values as a 1D series.

Now, set all DFT coefficients to zero except for this small region around this peak corresponding to the fringe lines, and inverse transform.

Single Patch Modal Analysis, always off

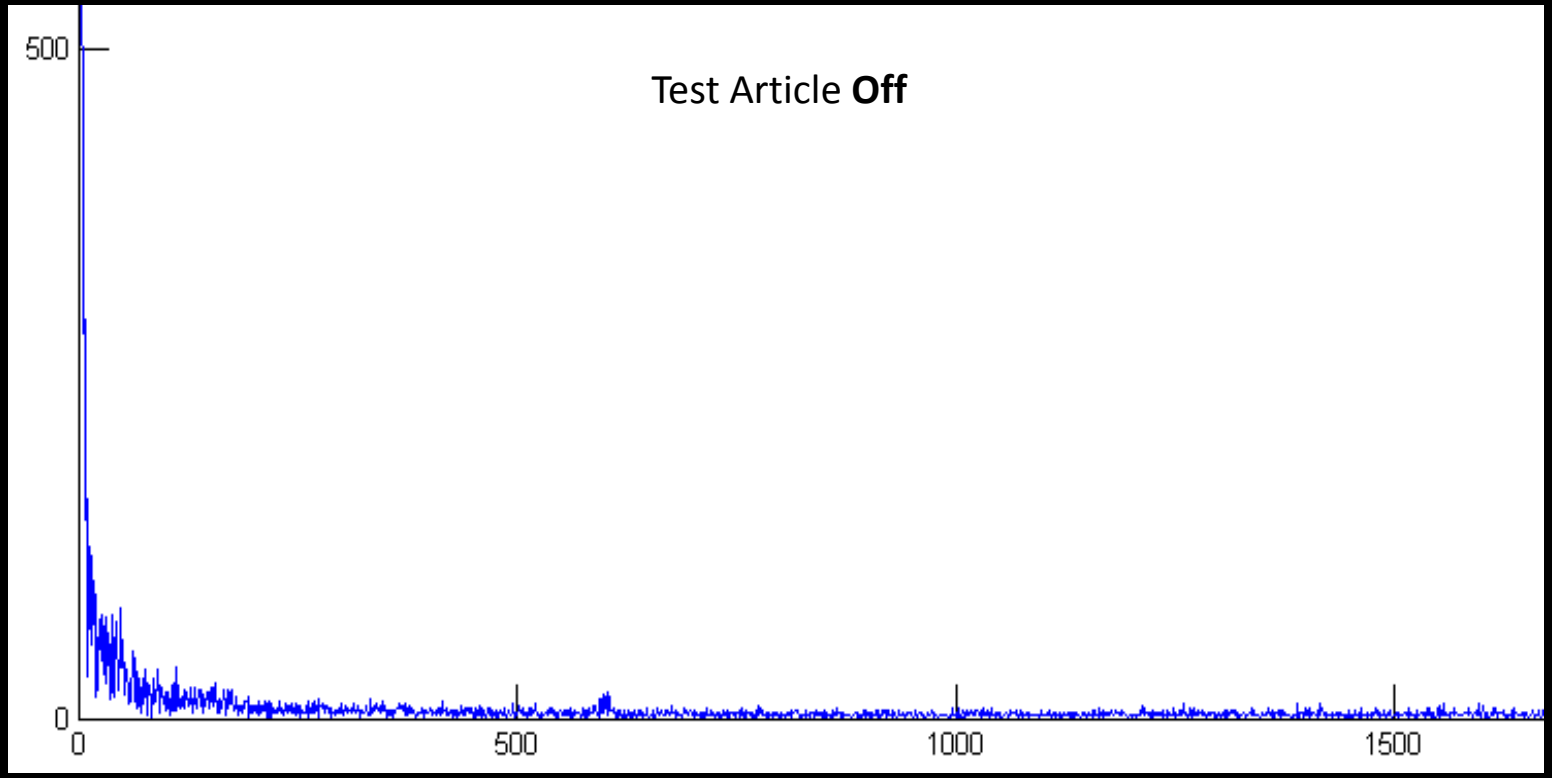

Magnitude Spectrum of Phase Series

Single Patch Modal Analysis, cycled on/off

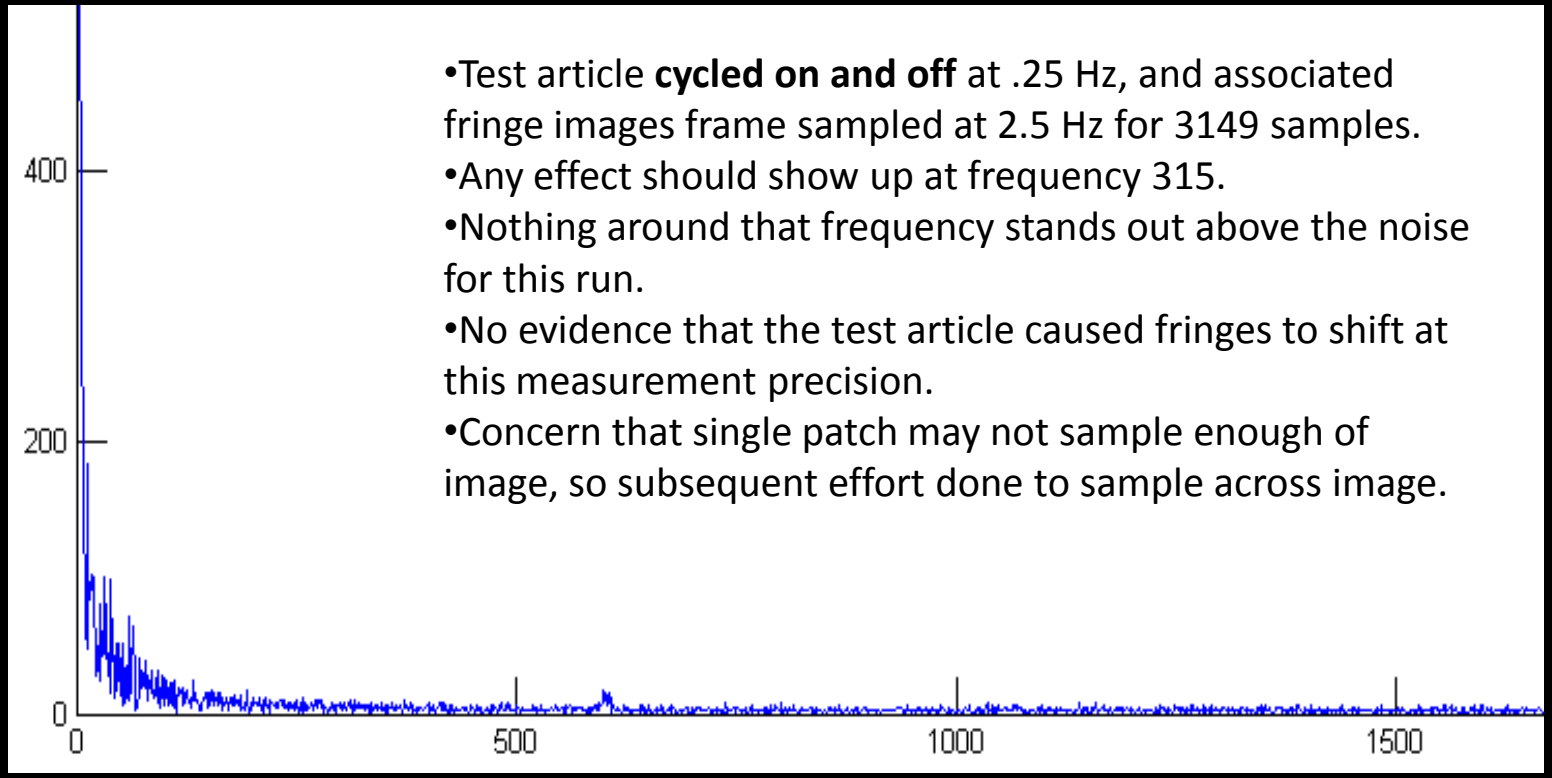

- Test article **cycled on and off** at .25 Hz, and associated fringe images frame sampled at 2.5 Hz for 3149 samples.
- Any effect should show up at frequency 315.
- Nothing around that frequency stands out above the noise for this run.
- No evidence that the test article caused fringes to shift at this measurement precision.
- Concern that single patch may not sample enough of image, so subsequent effort done to sample across image.

Magnitude Spectrum of Phase Series

MULTIPLE SAMPLE POSITIONS

INTERFEROMETER MODAL ANALYSIS, ANALYTIC SIGNAL VARIATION

Description of Work

- Room and table were floating
- Optical hood covering table
- Test article cycled on every 4 seconds
- Frames captured every 0.4 seconds
- 3149 frames processed
- Sampling occurred at 88 positions in image plane
- At each pixel sampled (through 3149 frames), the sample train was Fourier transformed, and the magnitude spectrum reviewed (see next slides)

Test Article Off

Magnitude Spectrum of Phase Series

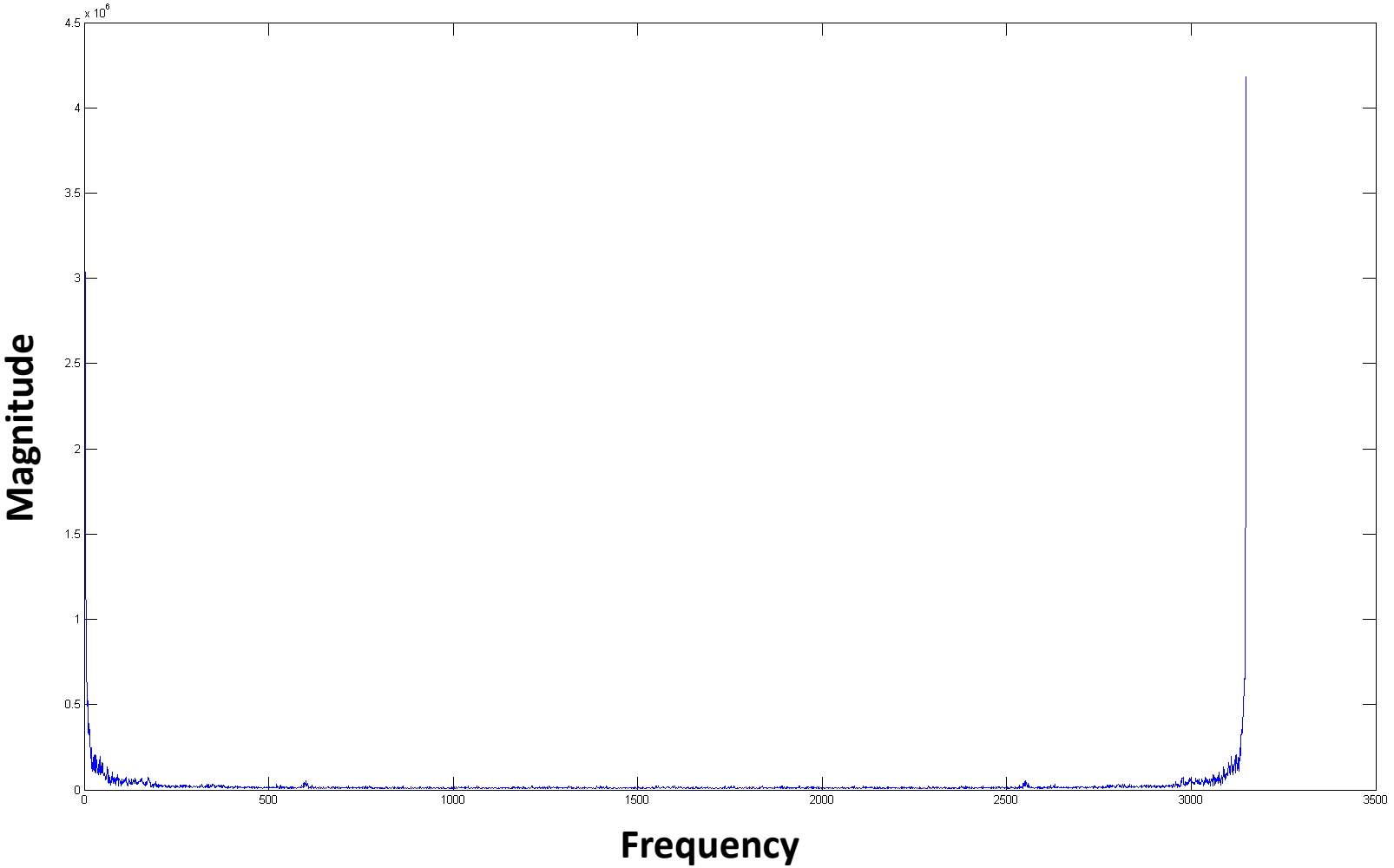

Test Article Cycled every 4 Sec (2 sec @ 20KV, 2 sec off)

Magnitude Spectrum of Phase Series

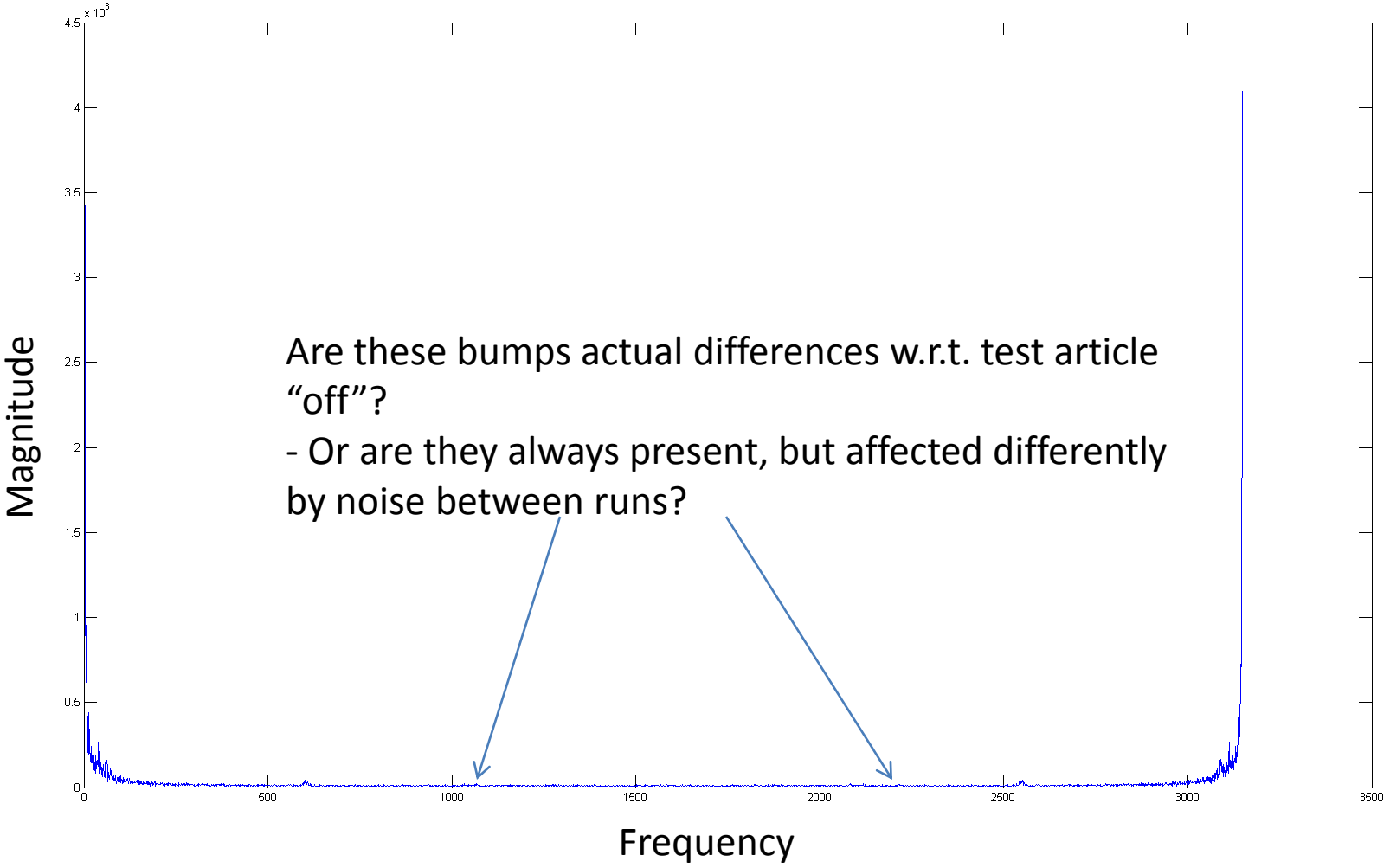

Close up (off)

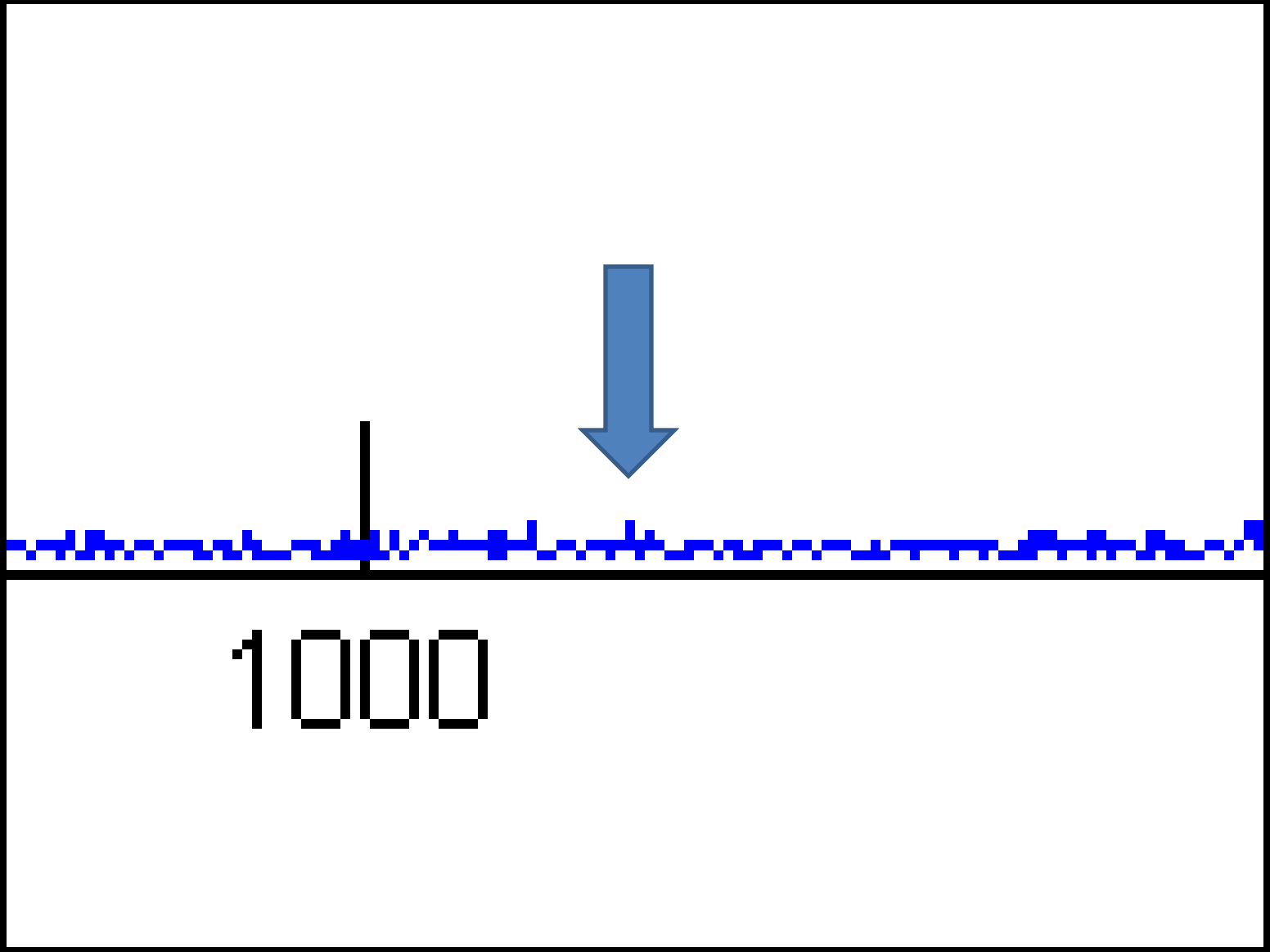

Close up (cycled)

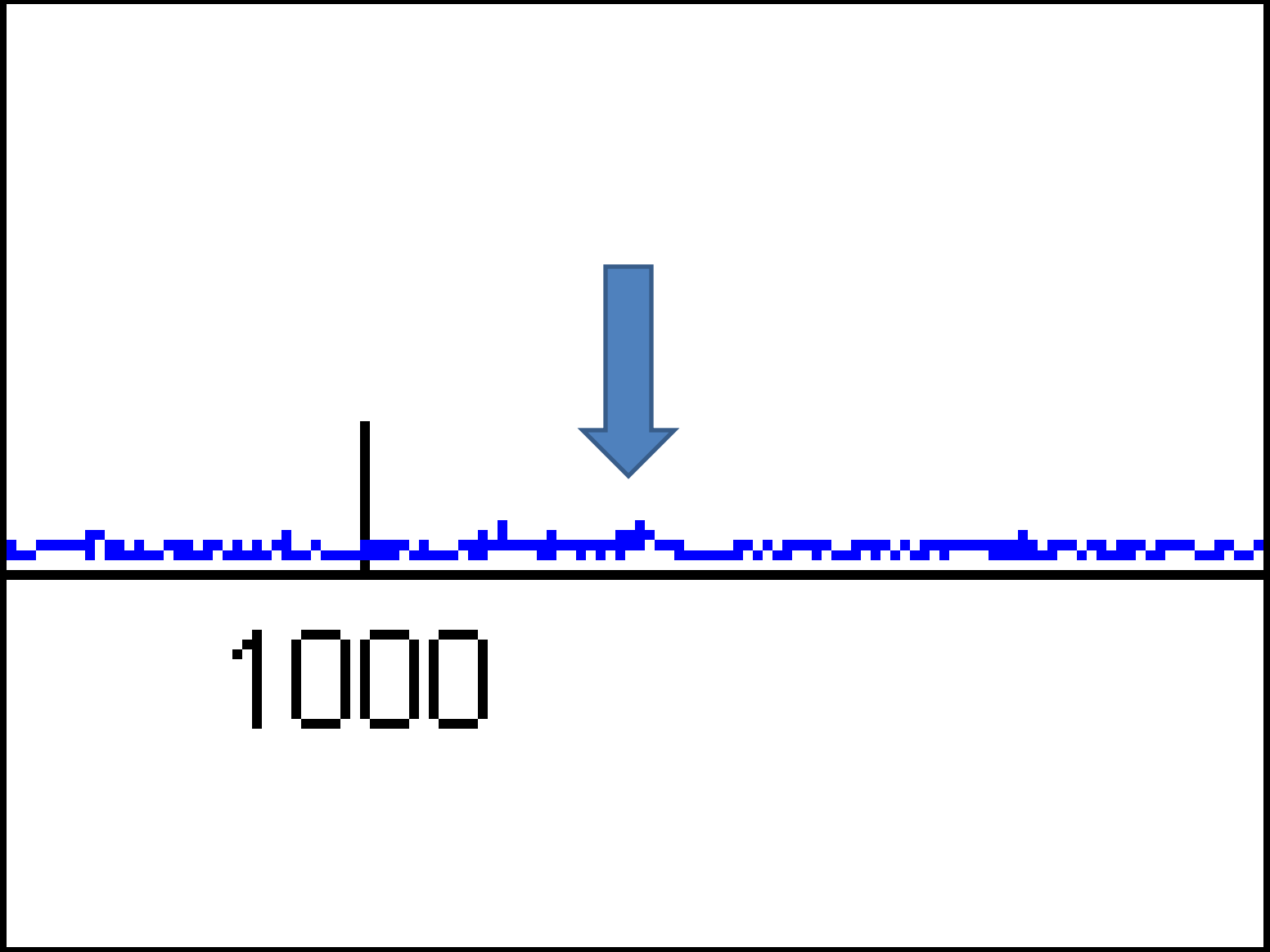

Air Dielectric in Beam Path

- Cap ring replaced with high-voltage device "Ozona" such that the charge collection sphere partially blocked the interferometer beam in the leg along the laser axis.
- High voltage source was cycled on and off in 2 second intervals.
- The screen capture was operating at a rate of 0.4 sec per frame.
- The optics table was floating but not the room.
- The optics table was not covered.
- HV source power strip was on the micro flat table next to the interferometer table.

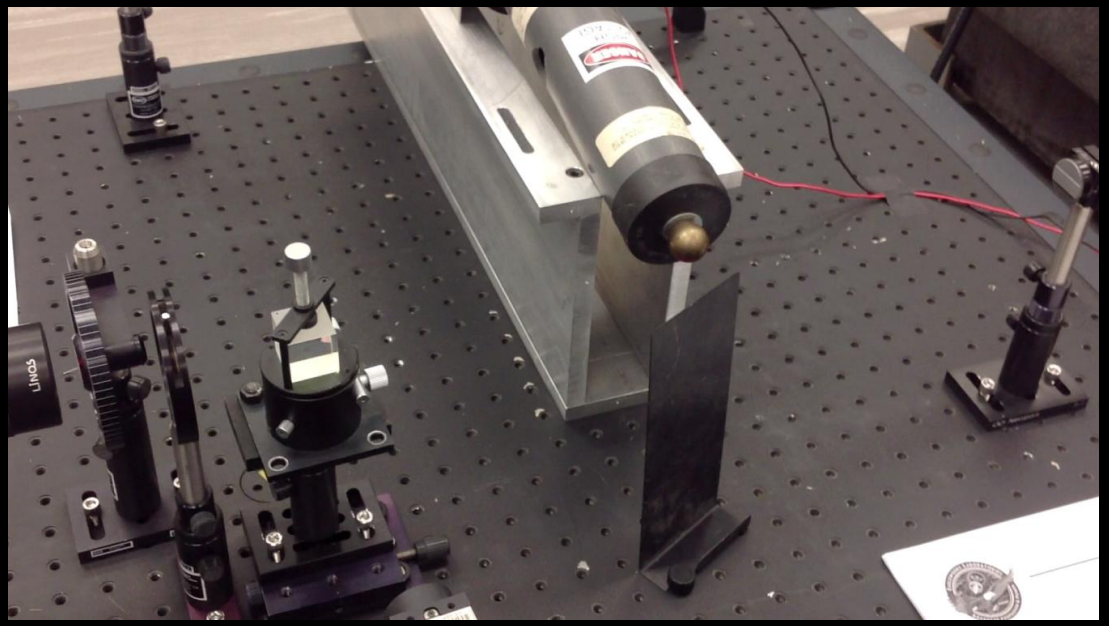

HV Power Supply Off

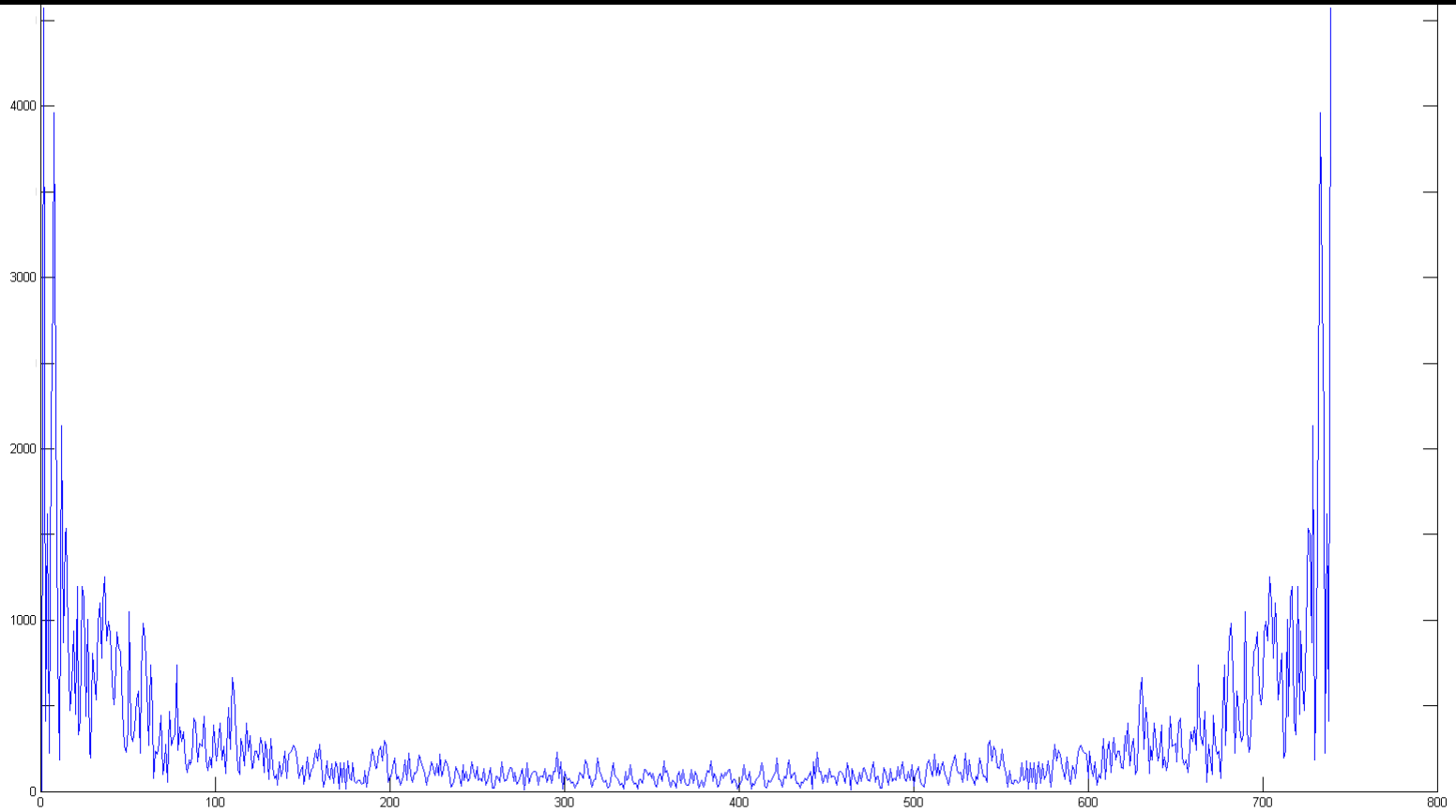

HV Power Supply Cycled @ 2 second Intervals

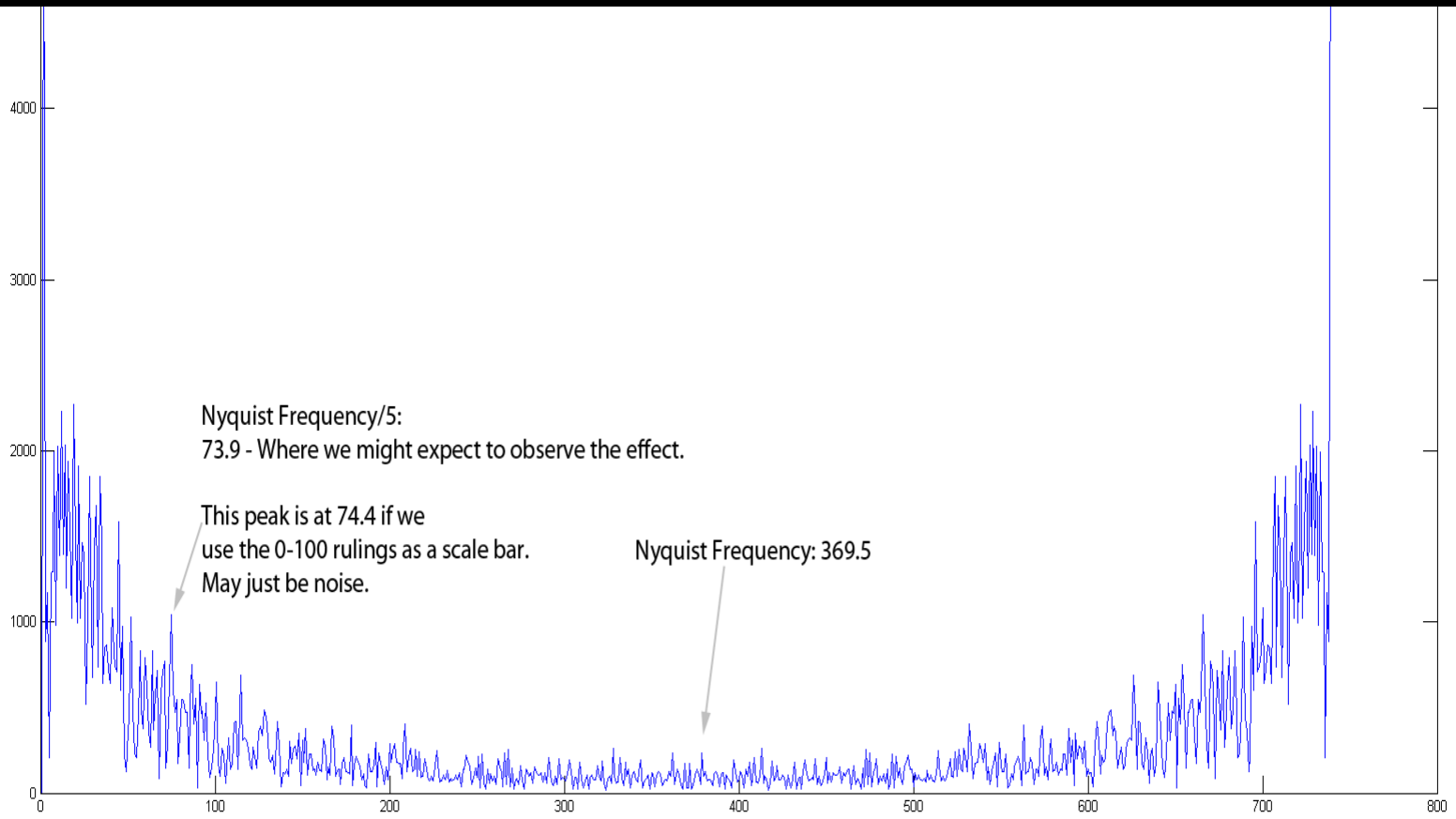

DAN NEHLICH, SOUTH DAKOTA STATE UNIVERSITY

INTERFEROMETRY MEASUREMENTS OF A DC TOROIDAL CAPACITOR

SDSU Interferometer Setup

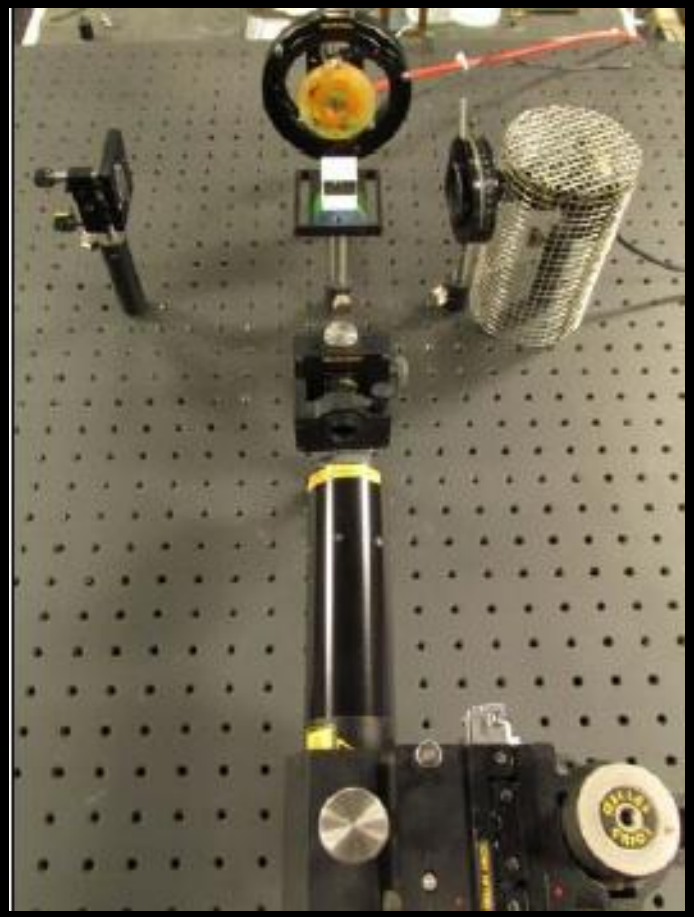

Warp Field Interferometer

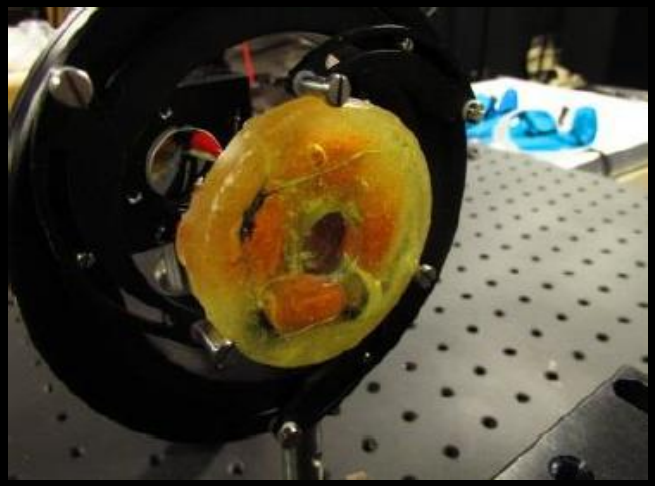

DC Toroidal Capacitor Test Article

Interference Pattern

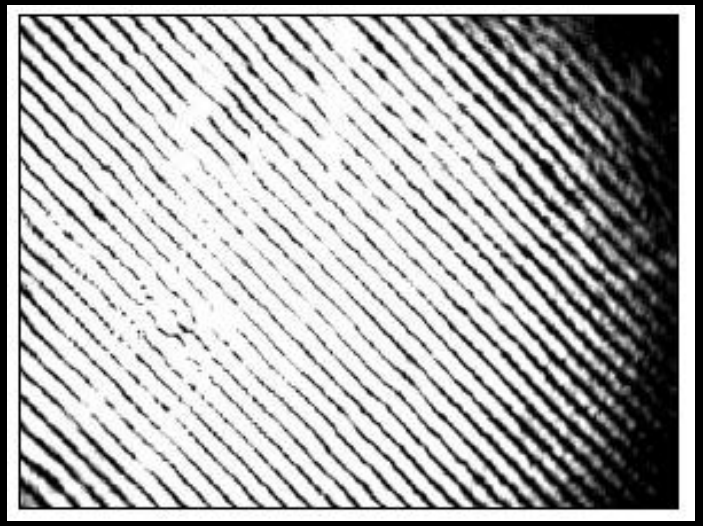

Image Subtraction Approach

- Positing that aberrations may include fringe pattern shifting in addition to or instead of induced curvature in the patterns, image subtraction was used to determine possible correlations to the voltage differential.
  - This method treats each image as an array and subtracts that array from the preceding, resulting in an image representative of the shift that occurred.
  - Average intensity of each subtracted image is calculated and statistical comparison is performed.
  - Statistical analysis of mean intensity values of each subtracted image, showed the observed shifts tended to increase during charge/discharge cycles, and remain constant in the control runs.
- The data presented in these scatter plots represents 2200 unique data points for charge/discharge cycles at 19 kV.
- Each point plotted represents approximately 20 images taken at the same point of the cycle, yielding an average intensity for each point in time along the graph.

Control, Charge, Discharge Scatter Plots

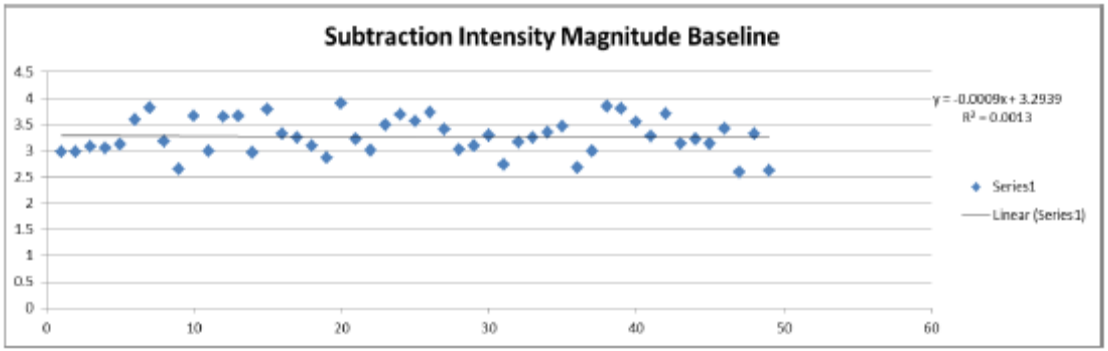

Figure 7: Image Subtraction with no charge/discharge present

control

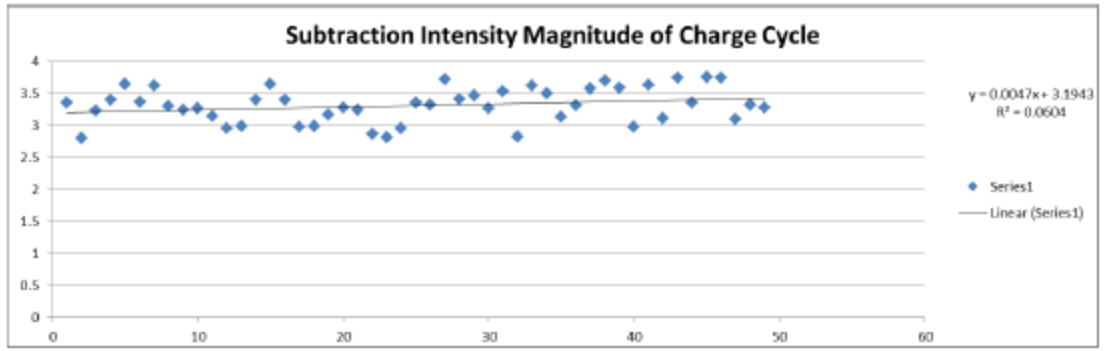

Figure 6: Image Subtraction during Test Article Charge Cycle from 0 V to 19 kV

charge

$$\frac{d\phi}{dt}?$$

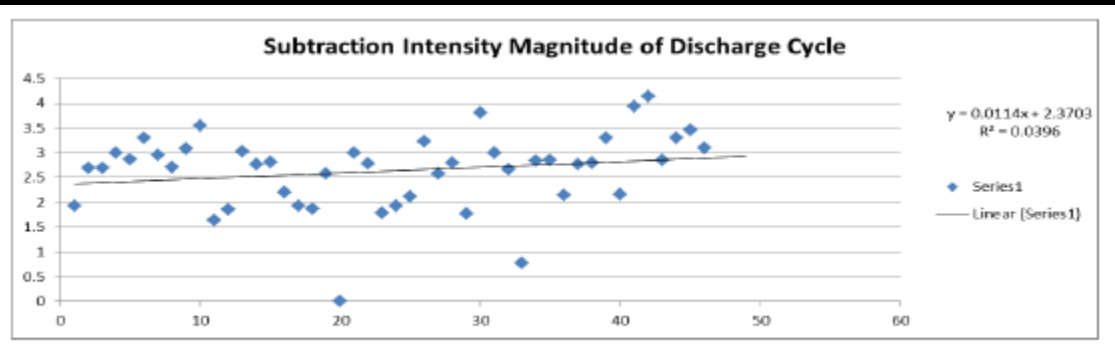

Figure 8: Image Subtraction during Test Article Discharge Cycle from 19 kV to 0 V

discharge

Hough Transform Approach

- In order to establish a direction of fringe pattern shifting, edge detection algorithms were necessary to determine individual line locations.
- The Hough Transform, along with the associated houghpeaks and houghlines functions in Matlab, was utilized to this end.
- An algorithm was written to utilize the edge mapping function of the transform, determine the distance of each line to the origin (normal to the fringe orientation) and then sort and weight the data to provide the relevant fringe locations for analysis.

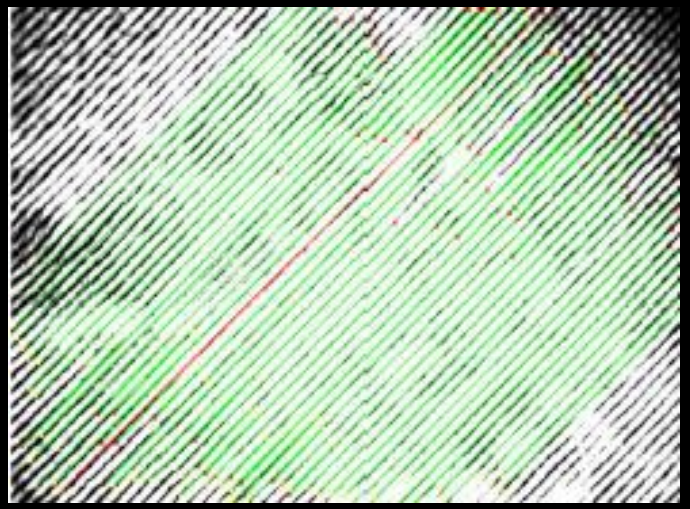

Hough Line Representation

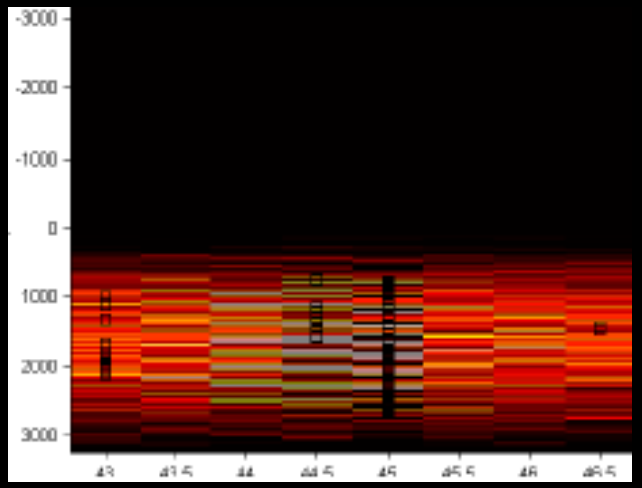

Hough Transform with Peaks

Cycle	Average Shift (pixels/frame)	St. Dev.	Average Shift -limited (pixels/frame)	St. Dev.
Control	0.050652543	1.652178	0.006819178	0.319178
Charge	-0.012880718	1.720073	0.010439022	0.341535
Discharge	0.005357819	0.810996	0.015817141	0.188845

Average Shifts of Interference Pattern

ENHANCED WARP FIELD PHYSICS EXPERIMENTS

IMAGE AVERAGING, FABRY-PEROT INTERFEROMETER, & TIME OF FLIGHT

Single Image

Averaged Image

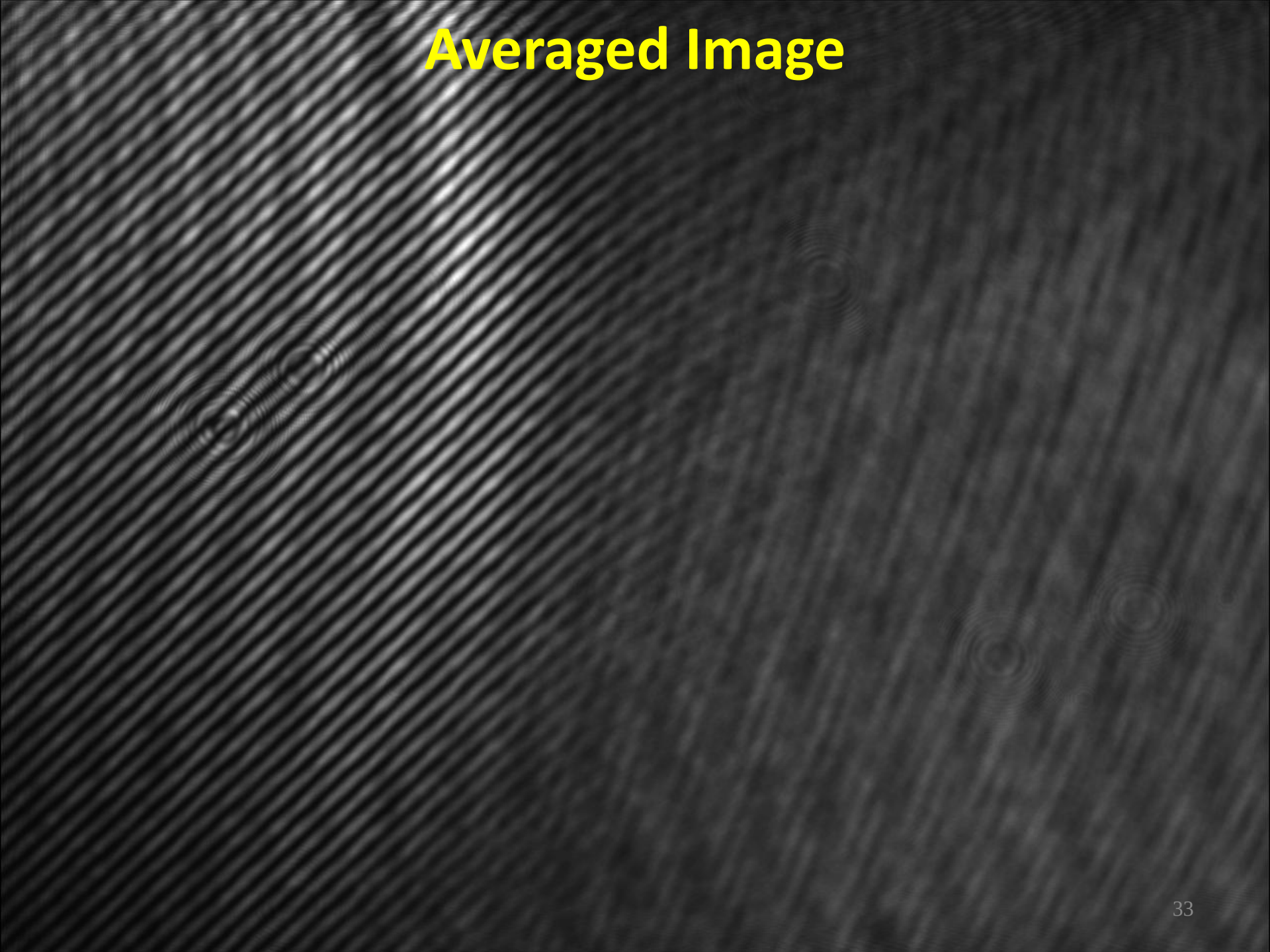

Fabry-Perot Warp Field Interferometer

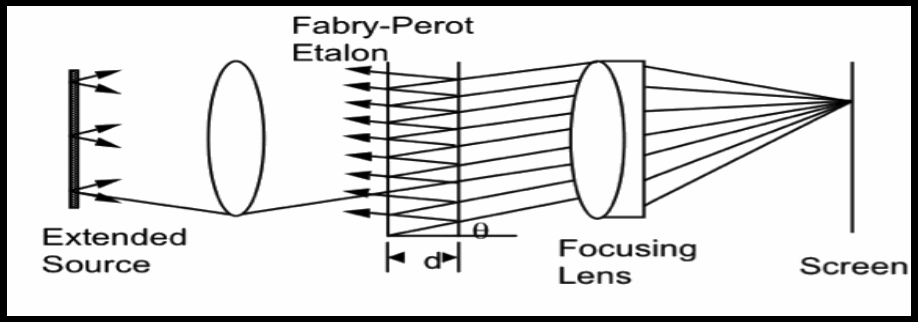

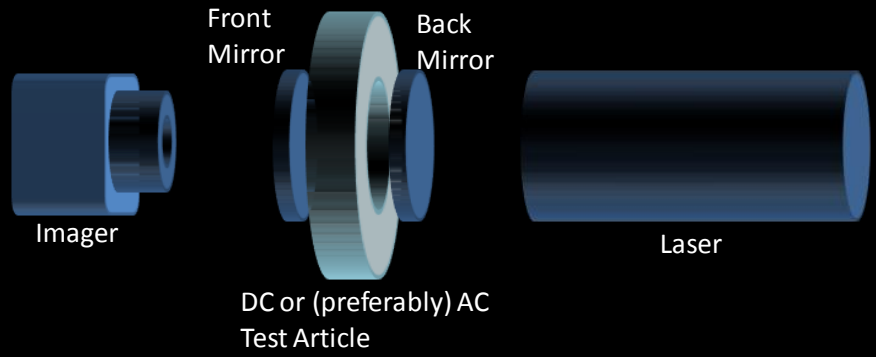

Example: Michelson-Morley Interferometer image for Sodium source

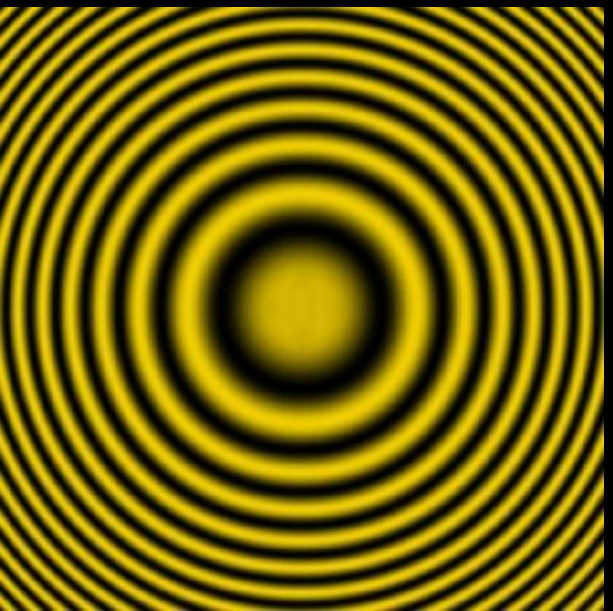

- Consists of two reflecting, highly parallel surfaces, called an Etalon
- The interference pattern is created within the Etalon
- Multiple reflections in the Etalon reinforce the areas where constructive and destructive interference occurs
- Allows for much higher-precision measurements of fringes (image averaging without software)

Example: Fabry-Perot Interferometer image for Sodium source (note doublet)

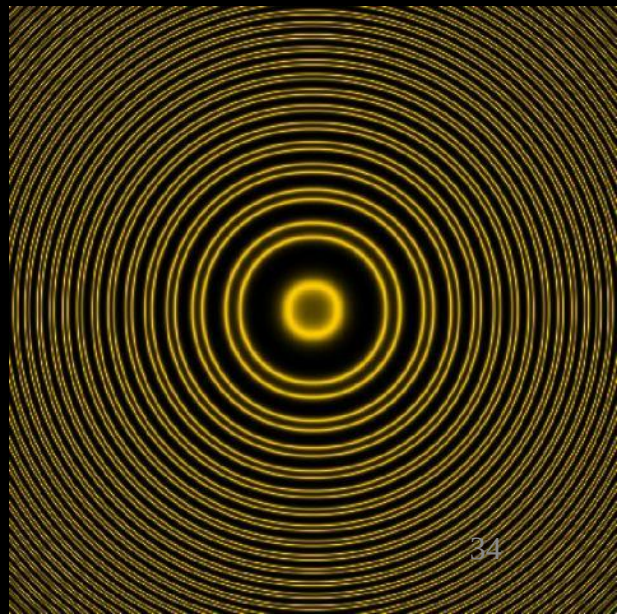

Fabry-Perot Experiment

He-Ne Laser

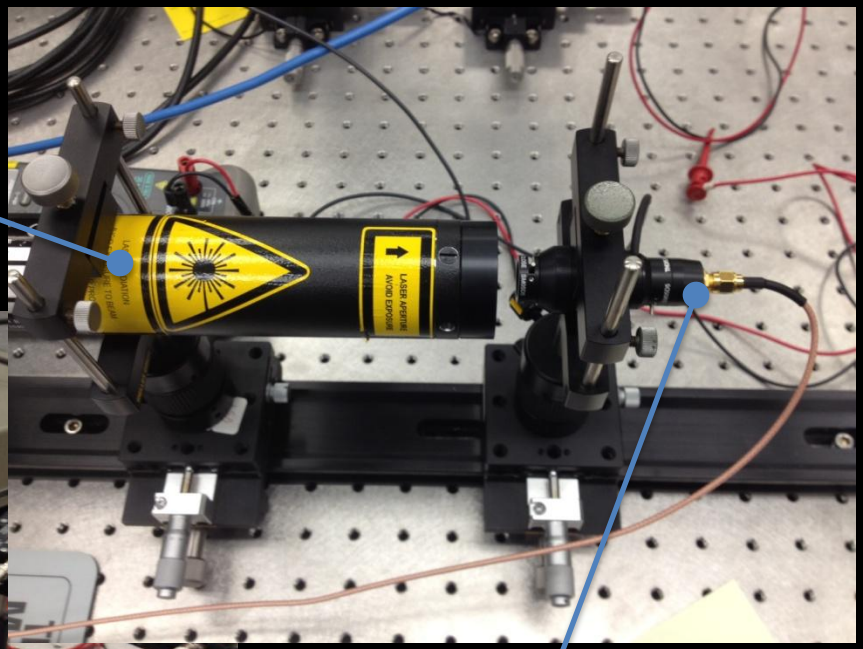

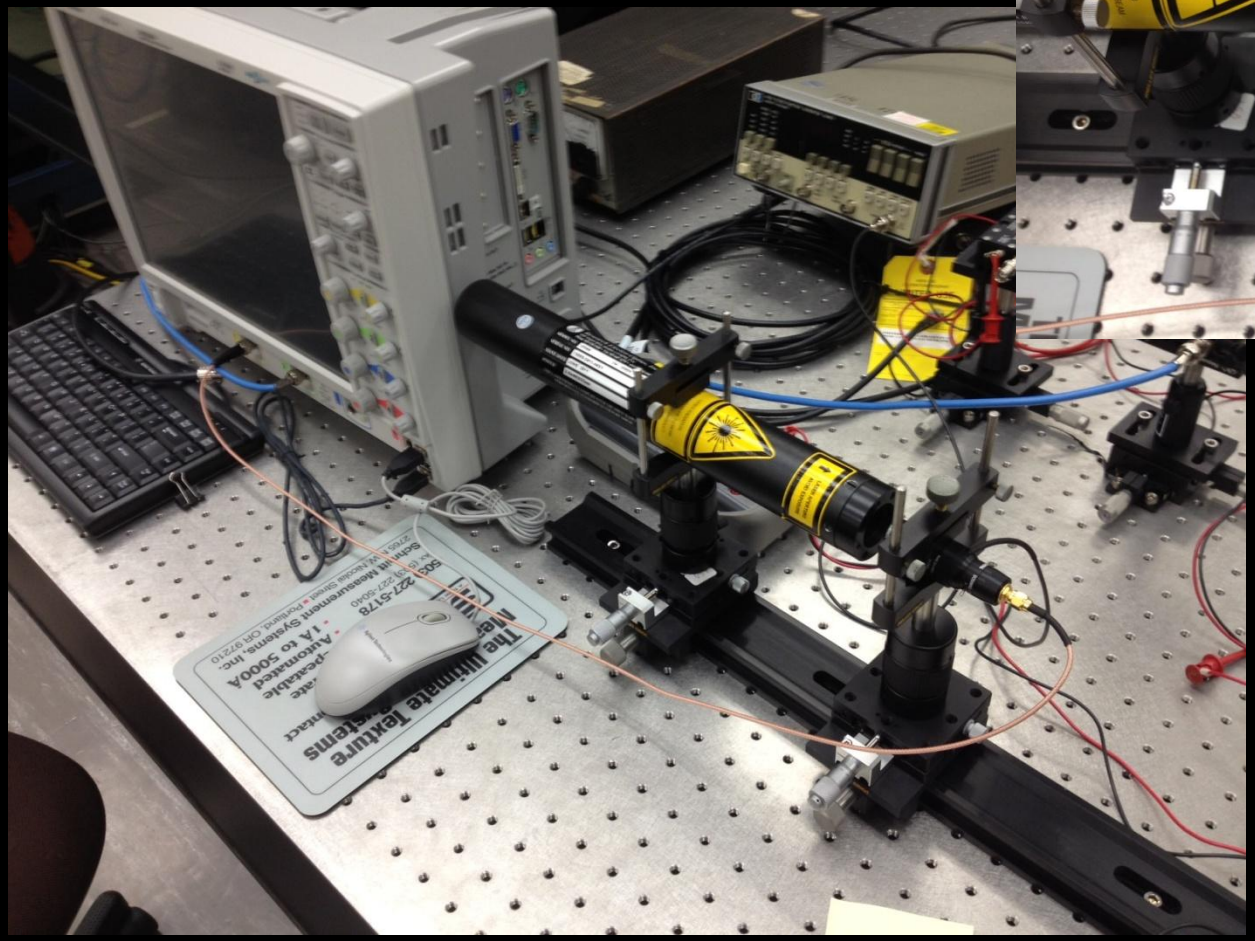

SA-210 Scanning Fabry-Perot Interferometer

Time of Flight Schematic

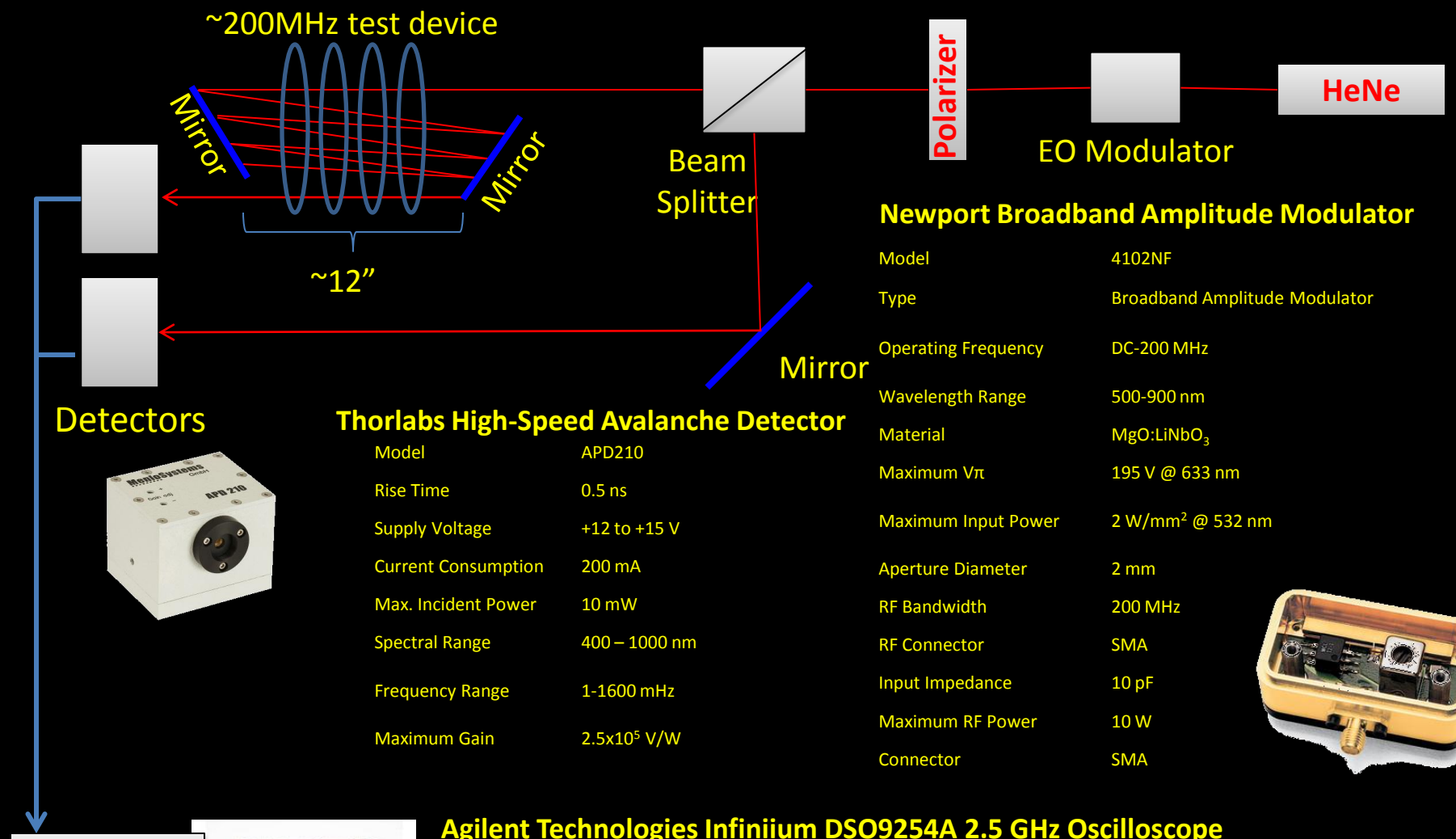

Thorlabs High-Speed Avalanche Detector

Model	APD210
Rise Time	0.5 ns
Supply Voltage	+12 to +15 V
Current Consumption	200 mA
Max. Incident Power	10 mW
Spectral Range	400 – 1000 nm
Frequency Range	1-1600 mHz
Maximum Gain	2.5×10^5 V/W

Newport Broadband Amplitude Modulator

Model	4102NF
Type	Broadband Amplitude Modulator
Operating Frequency	DC-200 MHz
Wavelength Range	500-900 nm
Material	$MgO:LiNbO_3$
Maximum Vπ	195 V @ 633 nm
Maximum Input Power	2 W/mm² @ 532 nm
Aperture Diameter	2 mm
RF Bandwidth	200 MHz
RF Connector	SMA
Input Impedance	10 pF
Maximum RF Power	10 W
Connector	SMA

Agilent Technologies Infiniium DSO9254A 2.5 GHz Oscilloscope

- 2.5 GHz bandwidth across all 4 analog channels
- 20 GSa/s max. sample rate
- Standard 20 Mpts memory per channel, upgradeable to 1 Gpts

Time of Flight Experiment

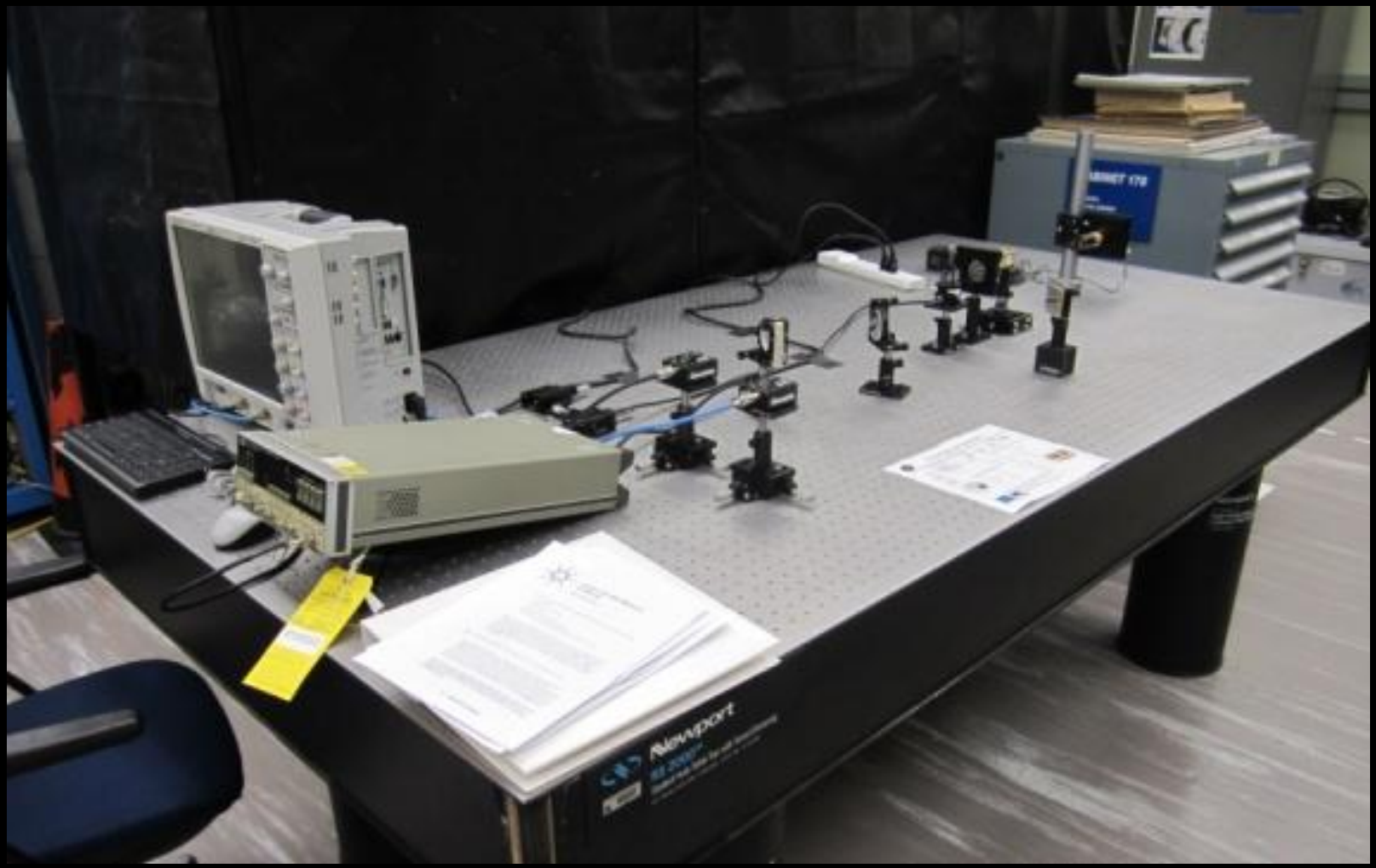

Forward Plan

- DC Toroidal Capacitor Approach:
  - Work with larger sample sets to decrease effects of vibrational “noise”, and develop test articles with longer regions of optical influence to increase the signal.
  - Utilize image averaging algorithms to increase fidelity of interference information.
  - Utilize the Fabry-Perot Interferometer to increase the sensitivity of the experimental apparatus to below 1/100 of a wavelength.

- Explore the $d\phi/dt$ dependency in future test devices
  - The idea of an optimized space warp needs negative vacuum energy, and large $d\phi/dt$ - both of these conditions are present in the q-thruster technology also being explored in the lab.
  - Use the q-thruster physics models to guide design of RF frequency test devices to be evaluated in the warp field interferometer, the Fabry-Perot Interferometer, and the time of flight experiment.

Q-Thruster

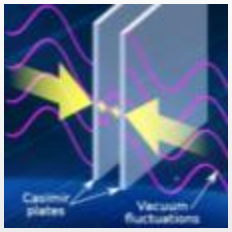

Casimir force

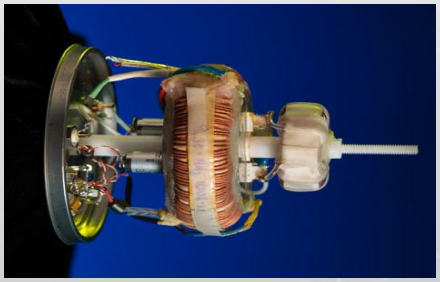

0.4N/kW test article

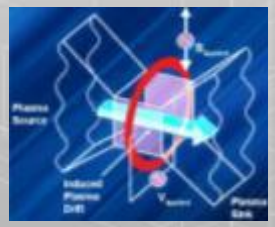

Quantum Vacuum MHD

- Q-thrusters are a low-TRL form of electric propulsion that operates on the principle of pushing off of the quantum vacuum.
- A terrestrial analog to this is to consider how a submarine uses its propeller to push a column of water in one direction, while the sub recoils in the other to conserve momentum – the submarine does not carry a "tank" of sea water to be used as propellant.
- In our case, we use the tools of Magnetohydrodynamics (MHD) to show how the thruster pushes off of the quantum vacuum which can be thought of as a sea of virtual particles - principally electrons and positrons that pop into and out of existence, and where fields are stronger, there are more virtual particles.
- The idea of pushing off the quantum vacuum has been in the technical literature for a few decades, but to date, the obstacle has been the magnitude of the predicted thrust which has been derived analytically to be very small, and therefore not likely to be useful for human spaceflight.
- Our recent theoretical model development and test data suggests that we can greatly increase the magnitude of the negative pressure of the quantum vacuum and generate a specific force such that technology based on this approach can be competitive for in-space propulsion (~0.1N/kW), and possibly for terrestrial applications (~10N/kW).
- As an additional validation of the approach , the theory allows calculation of physics constants from first principles: Gravitational constant, Planck constant, Bohr radius, dark energy fraction, electron mass.

Q-thruster Physics Data

2004 Test Article

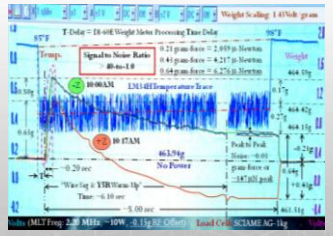

~4 mN Thrust
Specific Force ~0.4N/kW

1

2005 Test Campaign

The test unit was run at 2.13 MHz, yielding an AC electric field of ~20kV/m, and an AC magnetic field of ~27 Gauss.

- Based on the input parameters, the QVPT thrust prediction was 0.63 mN
- The observed thrust was +/- 0.89 mN

The test unit was run at 3.8 MHz yielding an AC electric field of ~20kV/m, and an AC magnetic field of ~48 Gauss.

- Based on the input parameters, the QVPT thrust prediction was 2.79 mN
- The observed thrust was +4.91 to -1.96 mN as measured via a 4900 mN (500gf) load cell

As can be seen to the right, the thrust signal is very clear when the unit is excited.

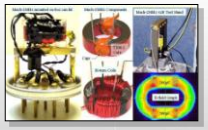

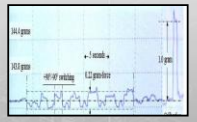

~3 mN Thrust
Specific Force ~0.3N/kW

2

2012 Test Article

2012 test article tested in November 2012

2012 test article tested -> 98uN predicted, 2-3 uN detected

- Scientifically very significant as vacuum fluctuation density had to be increased from ~1x10-26 to > 1x10-14
- As built quality factor much lower than desired, more engineering work necessary
- Adjustment to power distribution network are in work to address power losses, increase thrust level

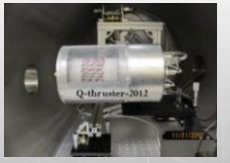

~vacuum fluctuation density increased from $1x10^{-26}$ to $>1x10^{-14}$

SFE Test Article at JSC

In 2013, Boeing/DARPA sent Eagleworks Lab an SFE test article for testing and evaluation

Evaluation of the test article in and out of a Faraday Shield performed from Feb through June 2013.

- There is a consistent transient thrust at device turn-on and turn-off that is consistent with Q-thruster physics
- The magnitude of the thrust scaled approximately with the cube of the input voltage (20-110uN).
- The magnitude of the thrust is dependent on the AC content of the turn-on and turn-off pulse
- Specific force of transient thrust was in the ~1-20 N/kW range.

SFE Test Article in Faraday Shield

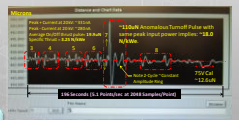

~20-110 uN Thrust Pulses
Specific Force ~1-20N/kW

5

Microwave Thruster Device

Aviation Week, 5 Dec 2012

Unreal Results?

Chinese academics say they have perfected the EmDrive thruster

SPR Ltd. Has produced several Microwave test articles. Claim is they produce thrust with just electric power input.

- Shawyer's theoretical model has been deemed non-viable by scientific community (rightly so)

Thruster assessed against Q-thruster models and analysis suggests this may be a microwave version of a quantum vacuum plasma thruster.

- Tapered shape creates virtual toroid of active volume that can realize net thrust in virtual plasma.
- Microwave Q-thrusters would not be restricted to tapered construction.

Thrust magnitude increased over multiple test devices from 16 to 170mN

If Q-Thruster theory accounts for measured force, then microwave test articles may have ability to reach >10N/kW

Chinese university claims to have duplicated EM Drive tests , but no way for U.S. to evaluate credibility (so we have ignored it)

Prototype 16mN @ 850W, 0.02N/kW

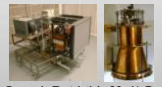

Dynamic Test Article 96mN @ 334W, 0.3N/kW

High fidelity Test Article 170mN @ 450W, 0.4N/kW

16-170 mN Thruster
Specific Force 0.02-0.4N/kW

6

Cannae Test Article

At DARPA's request, Eagleworks Lab began discussions with Cannae LLC on hosting a test article

Cannae's "Q-Drive" design is inspired by RF resonant cavity design used in particle linear accelerators

- Utilizes an asymmetric superconductive Niobium-Tin resonant cavity
- Cannae theoretical model is likely non-physical.

Initial assessment of conditions in thruster during operation indicate it may be a high frequency q-thruster.

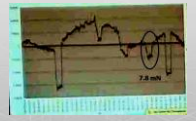

First Generation Test Article

Cannae Test Facility

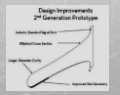

Second Generation Test Article (under development)

~7-10 mN Thruster
Specific Force ~0.75N/kW

7

What we suspect:

- A variety of industry experiments, for which theory is lacking, may be Q-thrusters including Boeing, Lockheed-Martin, EM Drive, Cannae, etc.
- Low measured thrust but specific power ranges from 0.3 to 10+ N/KW

Q-thruster Roadmap

~10N/kW

High altitude, high speed aircraft

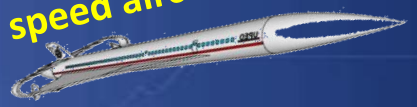

Lox, LCH4 fed turbines power banks of q-trhrusters

High thrust, high Isp spacelift (2000s effective specific impulse)

In-space
Space-lift
Aero

Blimp Test

Deep Space Exploration

?N/kW

In-space

Space Tugs

ISS Free Flyer
COTS Free Flyer
Class D Mission

~0.1N/kW

Outer solar system exploration & beyond

Fast Mars missions

Q-THRUSTER + 2MW NUCLEAR POWER IS MISSION ENABLING

POSSIBLE MISSIONS TO MARS, THE OUTER SOLAR SYSTEM, AND BEYOND WITH Q-THRUSTERS

Mars

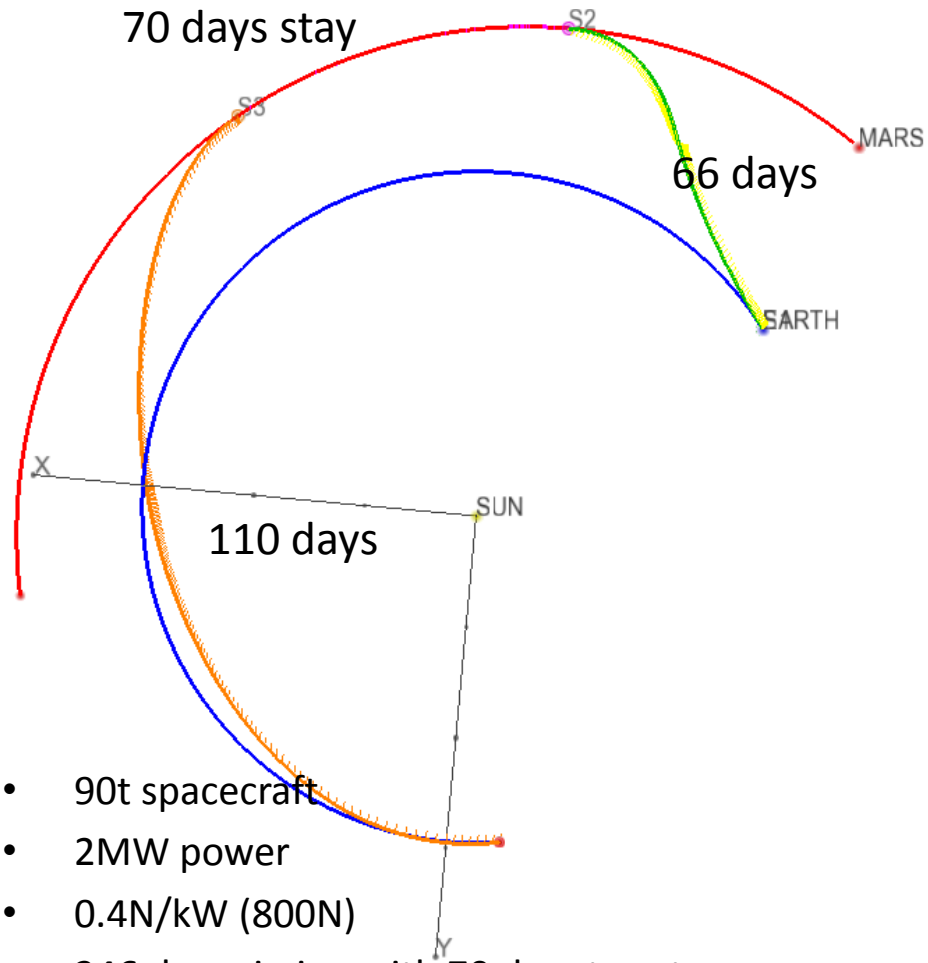

- 90t spacecraft
- 2MW power
- 0.4N/kW (800N)
- 246 day mission with 70 day stay at Mars

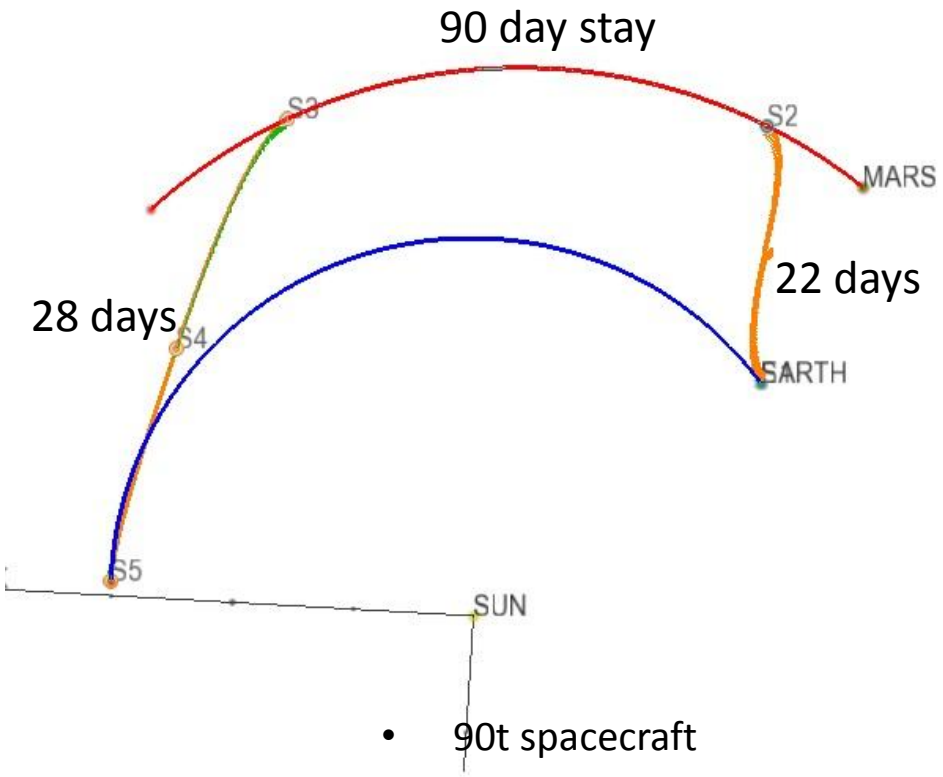

- 90t spacecraft
- 2MW power
- 4N/kW (8000N)
- 140 day mission with 90 day stay at Mars

Jupiter

0.4 N/kW

194 days

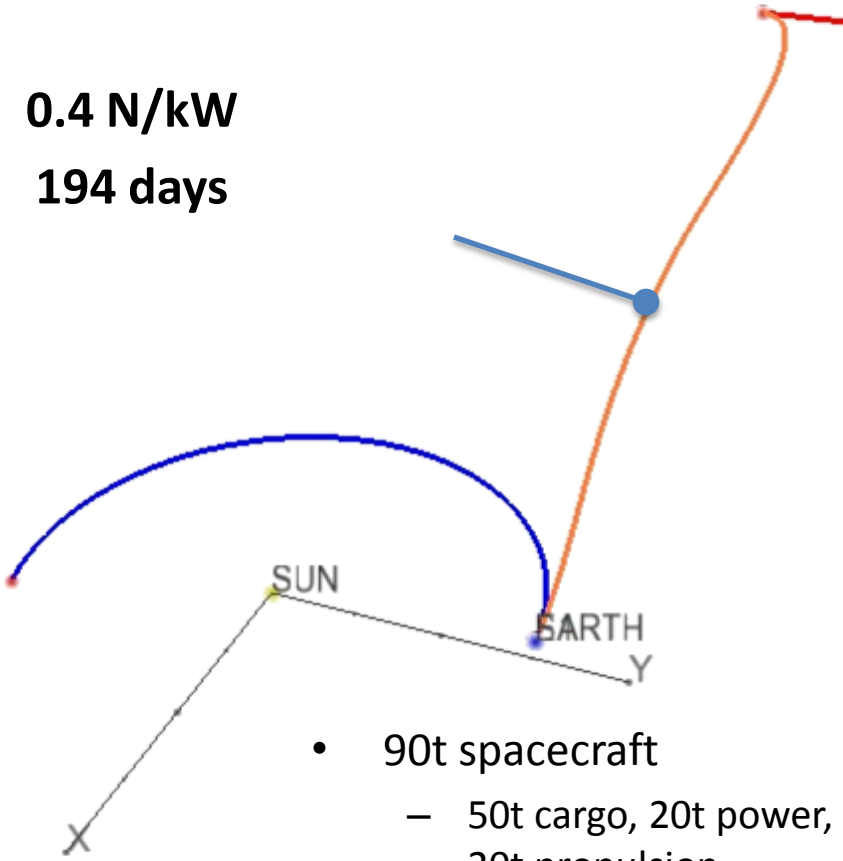

4 N/kW

61 days

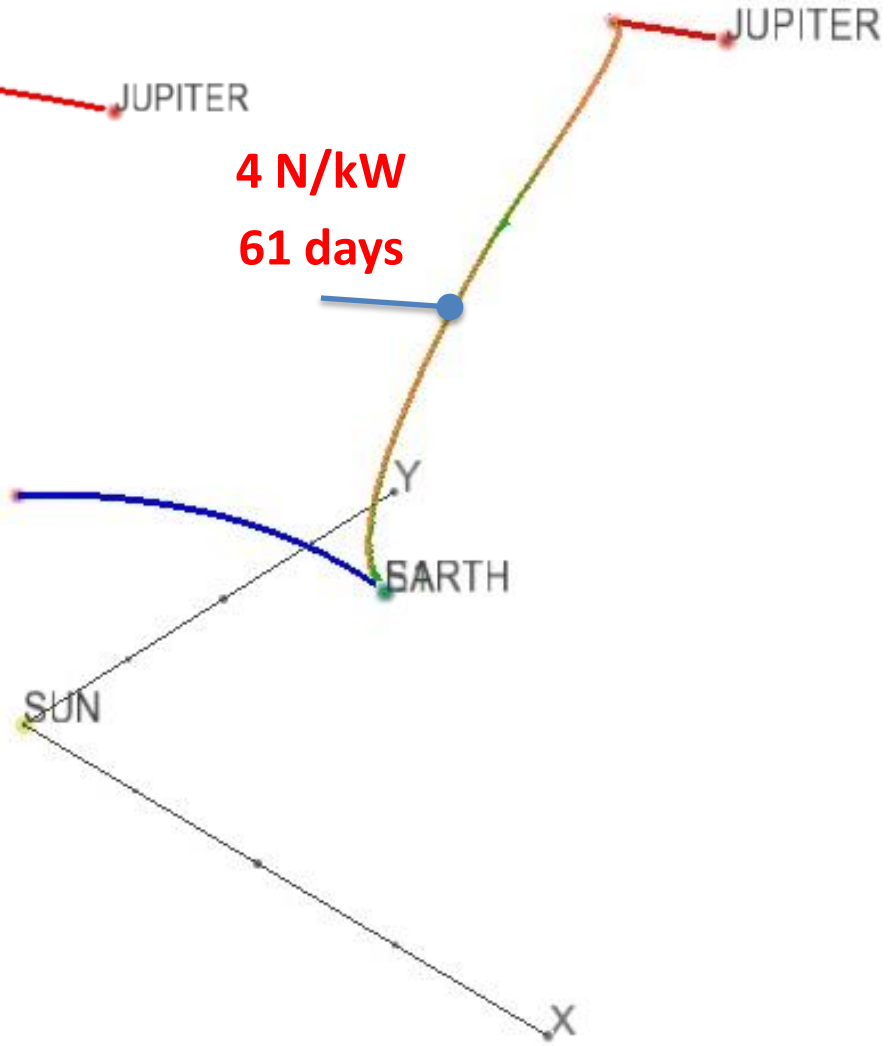

- 90t spacecraft
  - 50t cargo, 20t power, 20t propulsion
- 2MW power

Saturn

0.4 N/kW

263 days

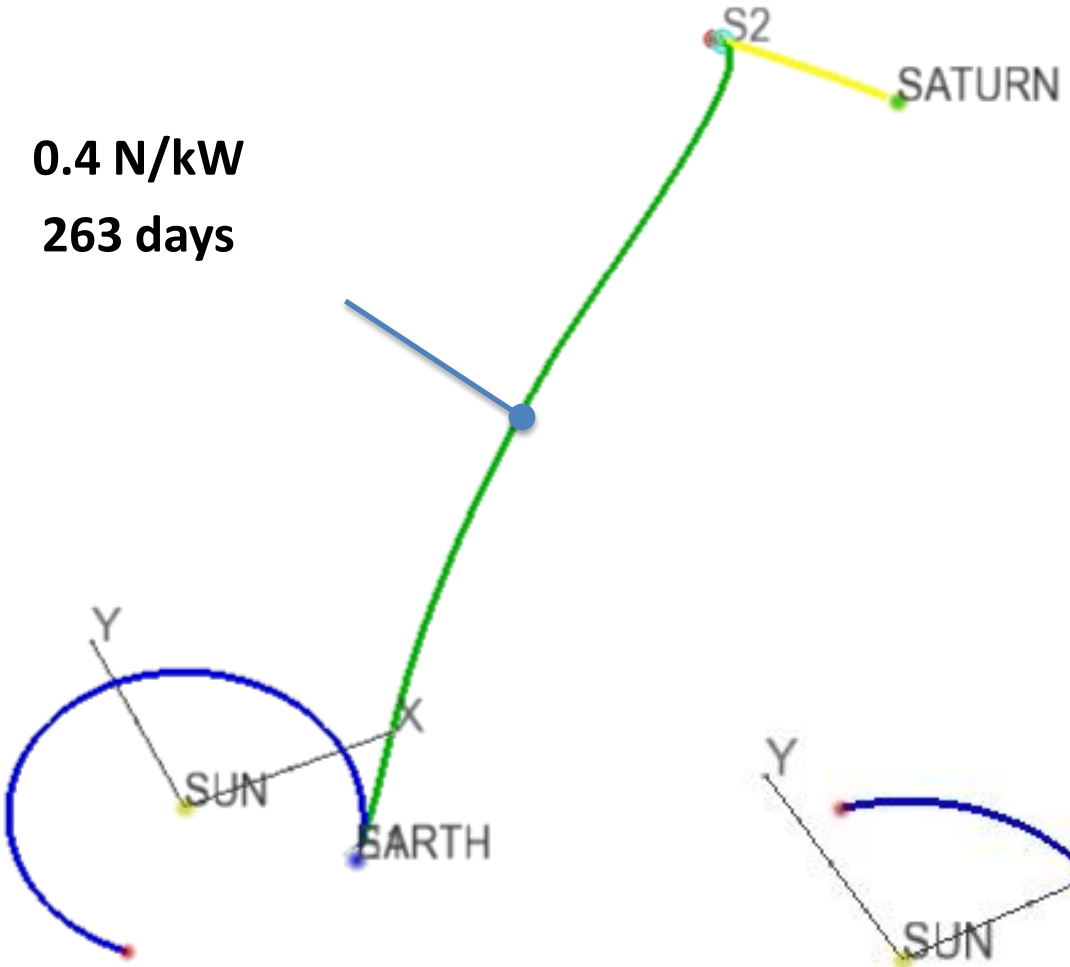

4 N/kW

86 days

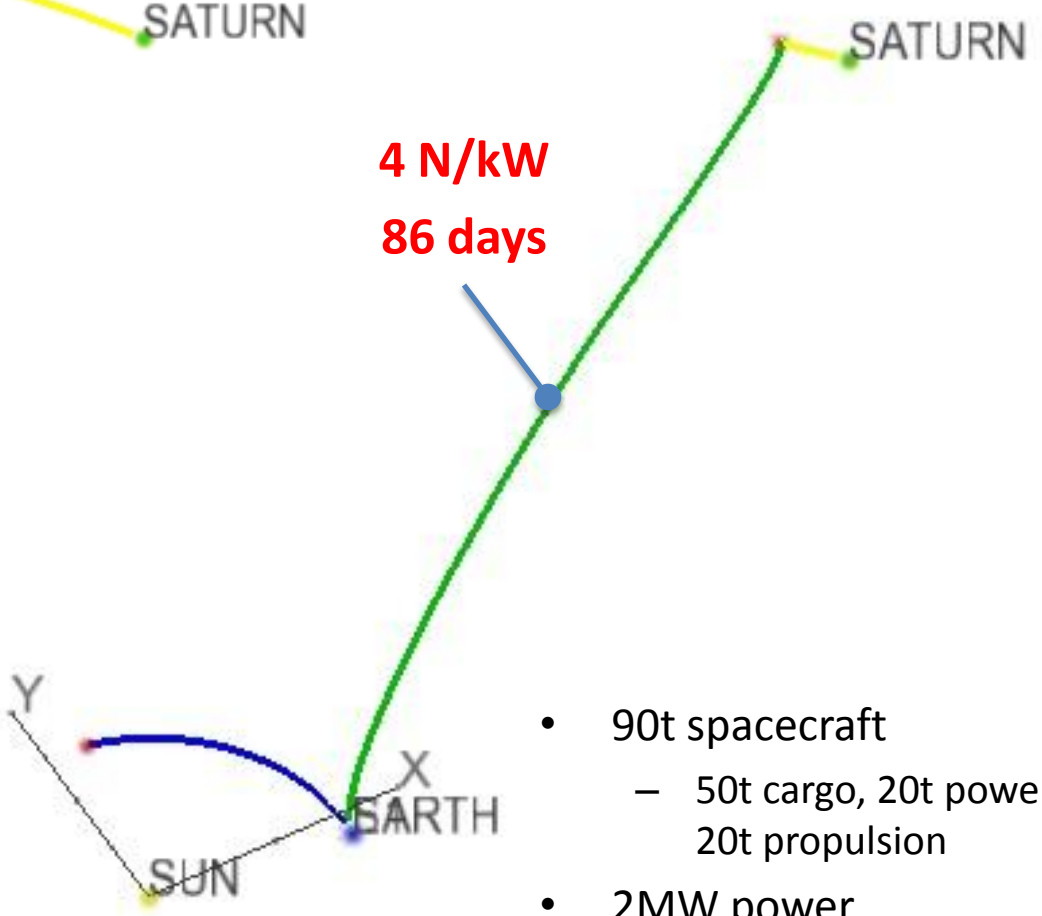

- 90t spacecraft
  - 50t cargo, 20t power, 20t propulsion
- 2MW power

Uranus

0.4 N/kW

399 days

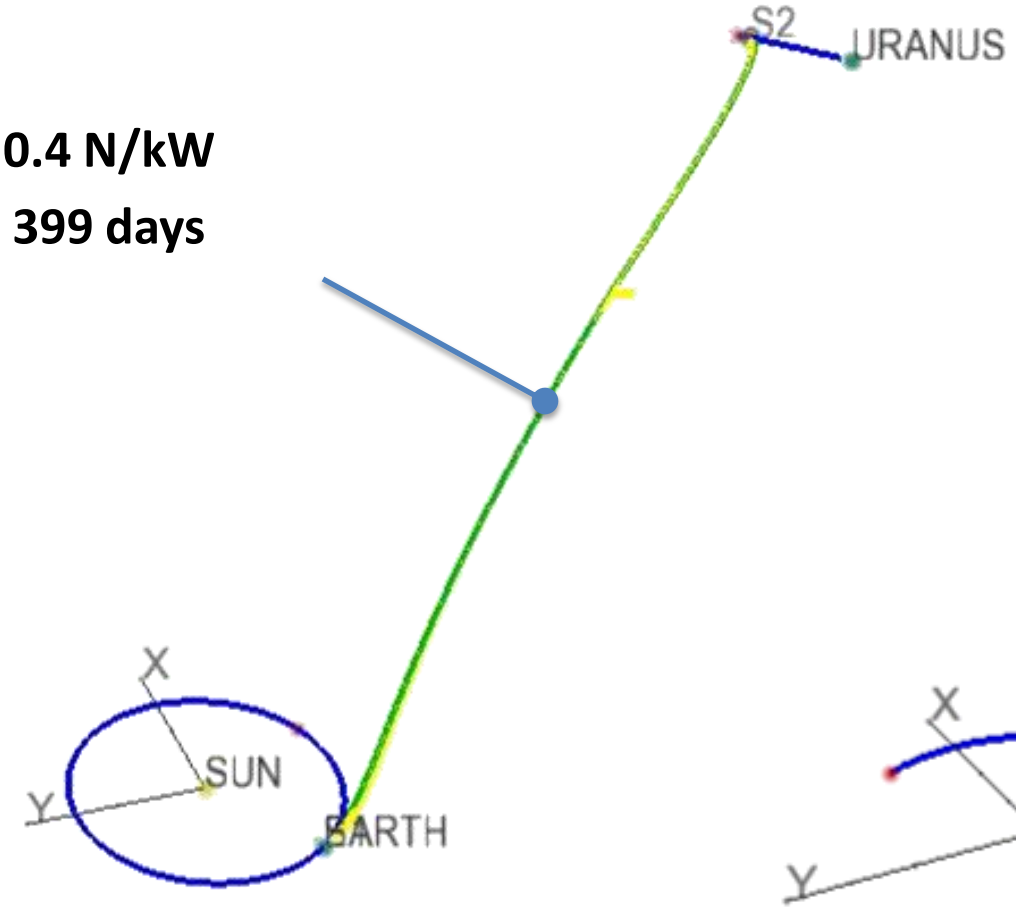

4 N/kW

129 days

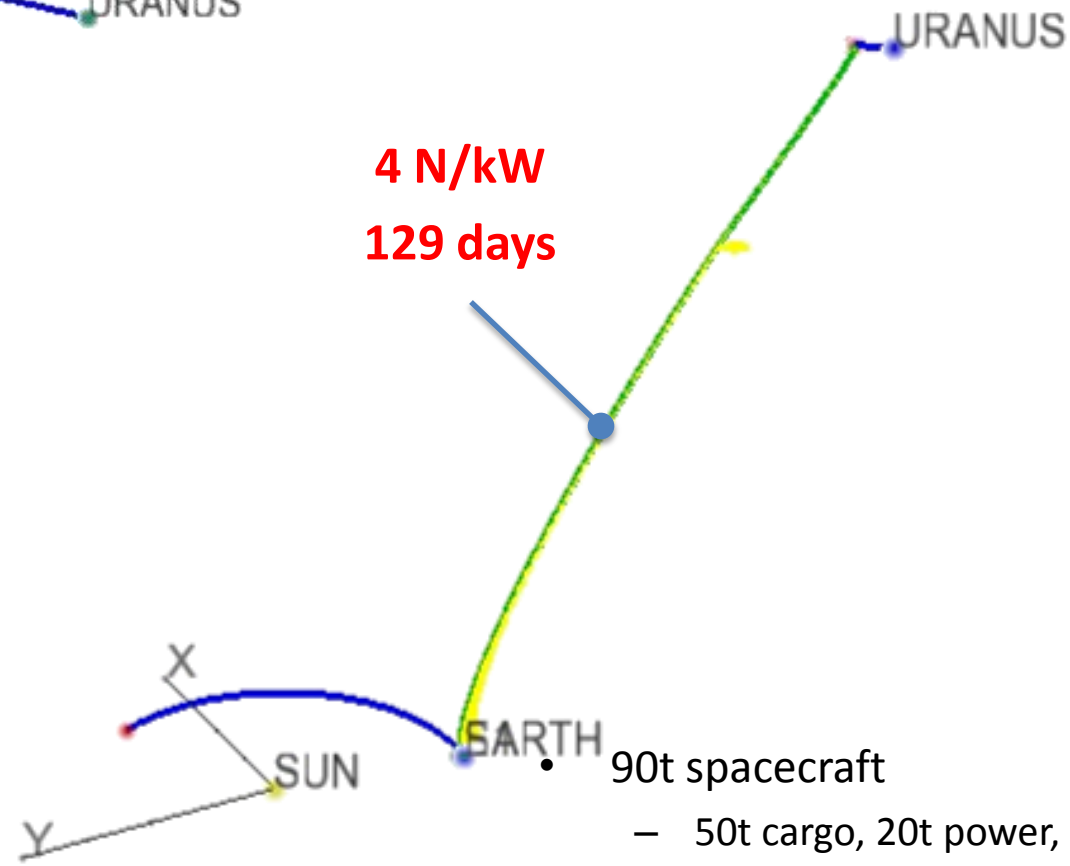

- 90t spacecraft
  - 50t cargo, 20t power, 20t propulsion
- 2MW power

Neptune

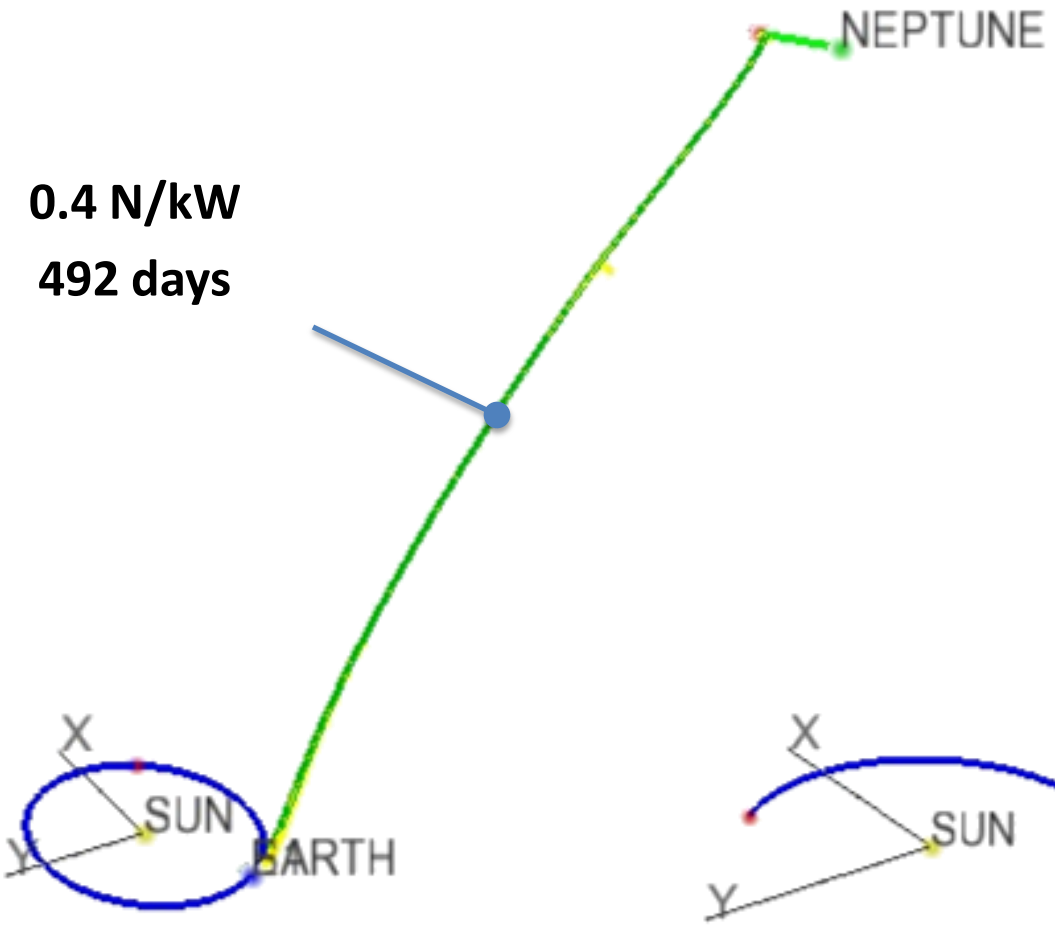

0.4 N/kW

492 days

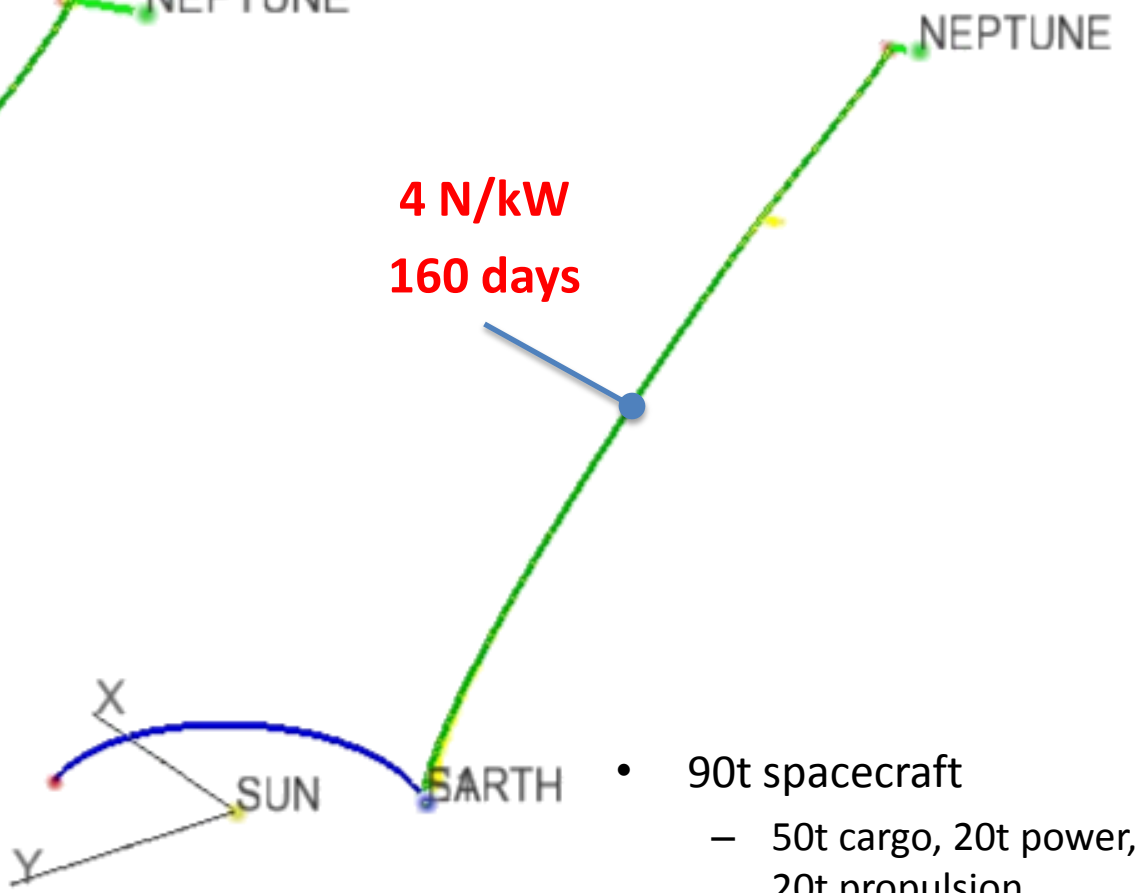

4 N/kW

160 days

- 90t spacecraft
  - 50t cargo, 20t power, 20t propulsion
- 2MW power

Pluto

0.4 N/kW

518 days

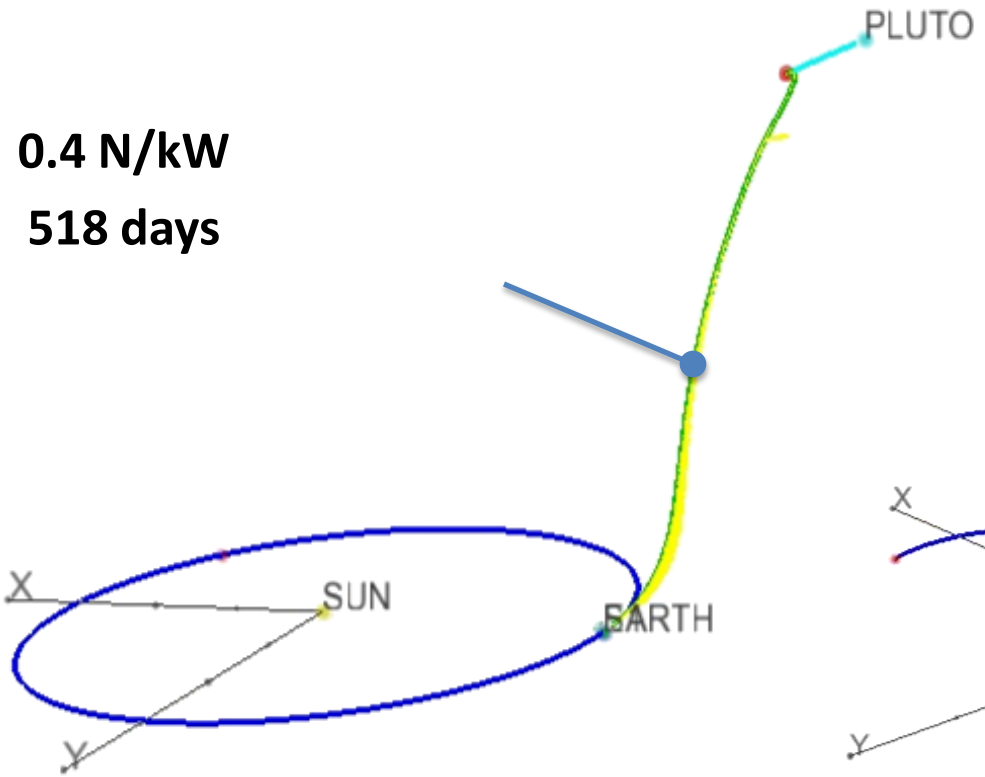

4 N/kW

167 days

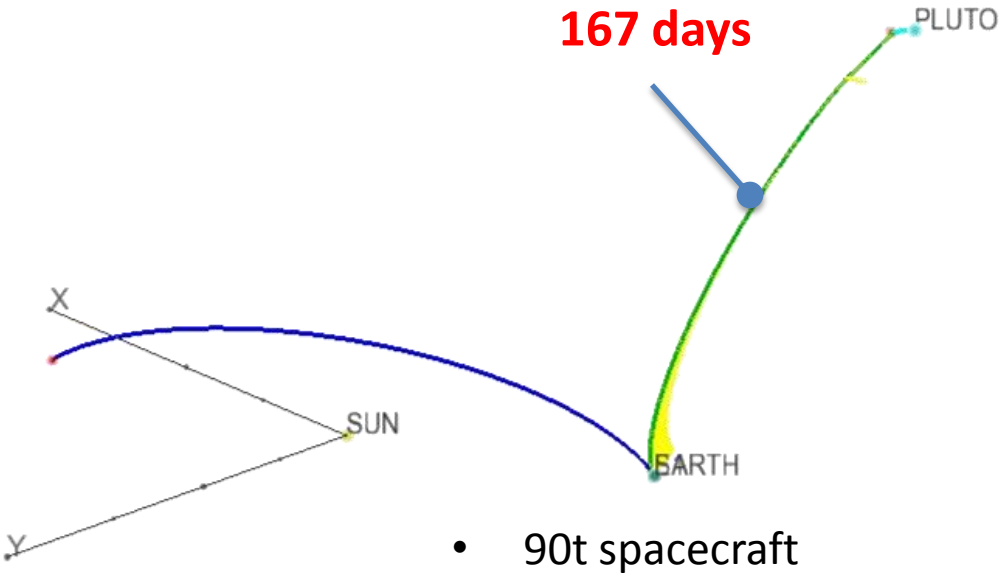

- 90t spacecraft
  - 50t cargo, 20t power, 20t propulsion
- 2MW power

1000 AU

0.4 N/kW

5.6 years

4 N/kW

1.8 years

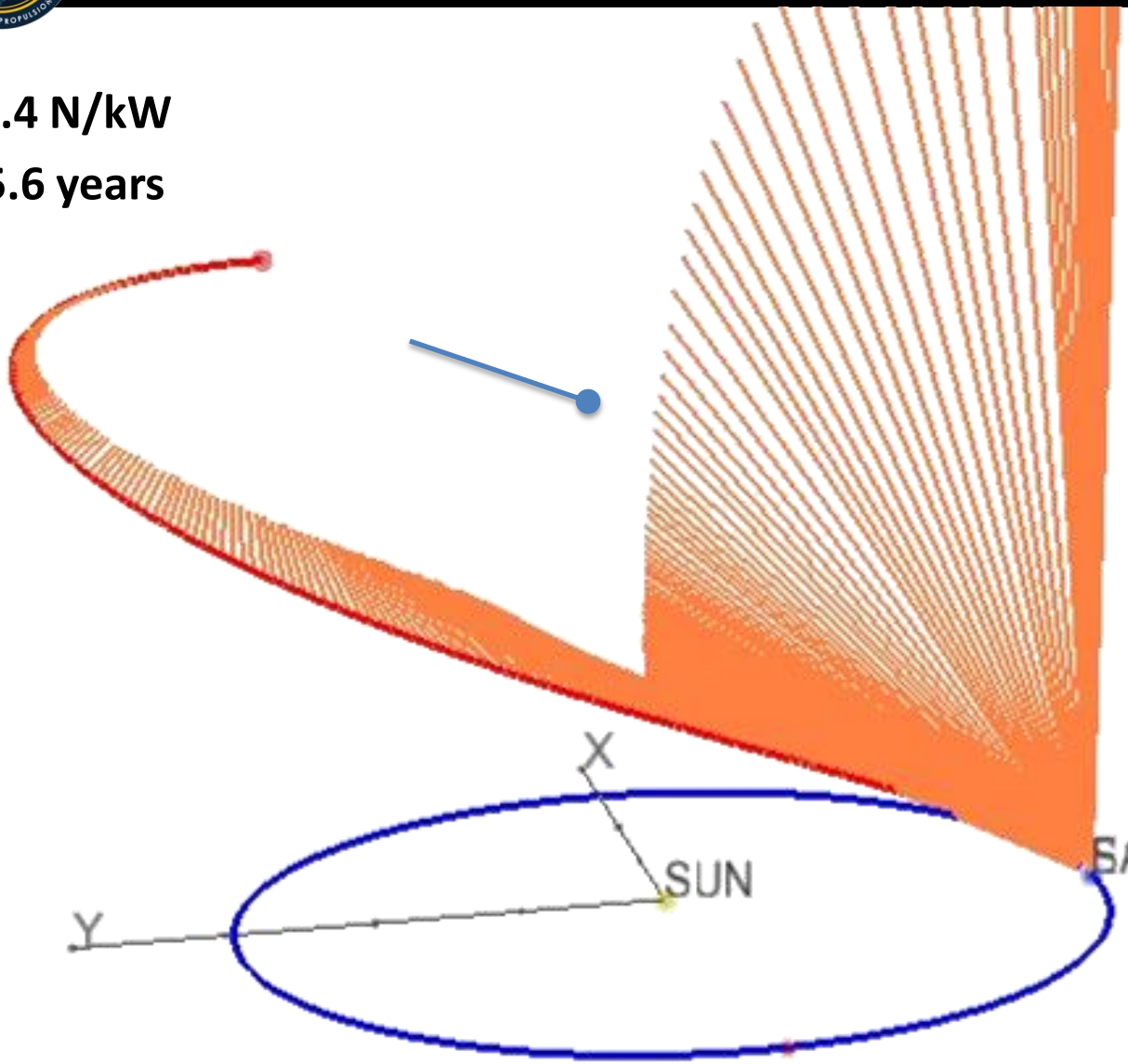

- 90t spacecraft
  - 50t cargo, 20t power, 20t propulsion
- 2MW power

PROXIMA CENTAURI

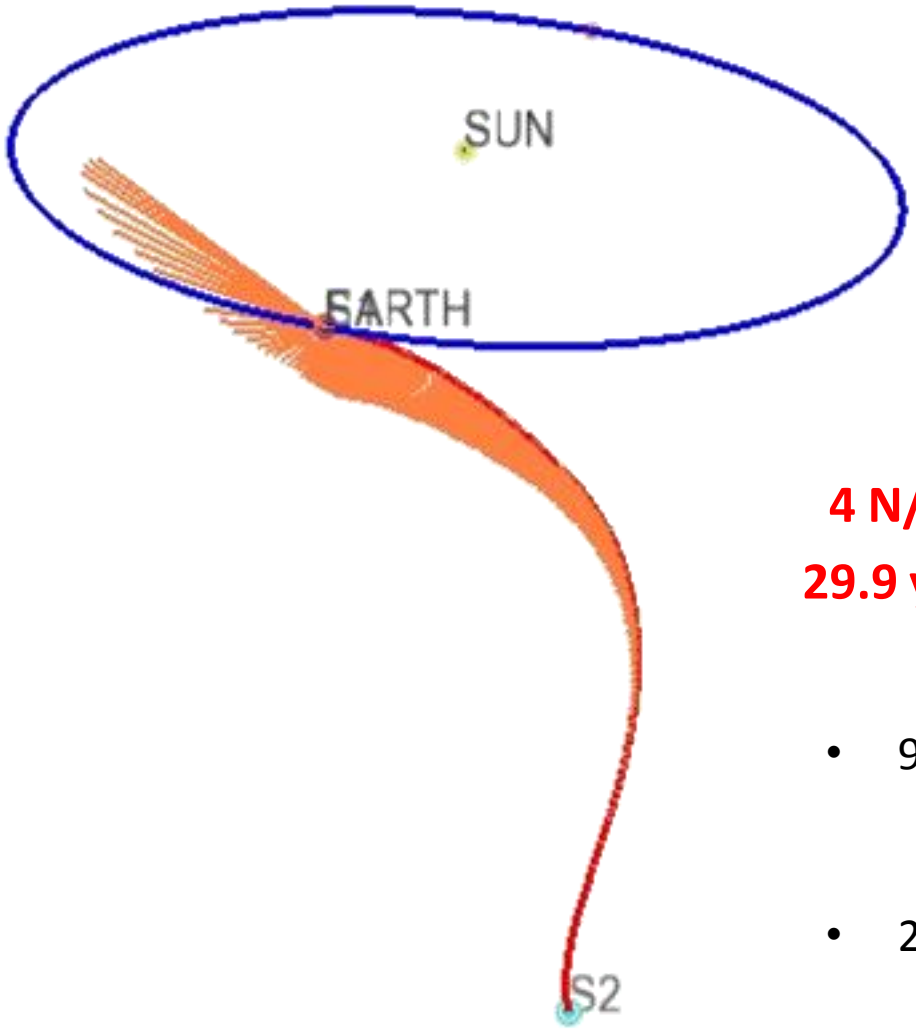

0.4 N/kW

122.5 years

4 N/kW

29.9 years

- 90t spacecraft
  - 50t cargo, 20t power, 20t propulsion
- 2MW power

Original Matthew Jeffries concept from mid 1960's, rendered by Mark Rademaker

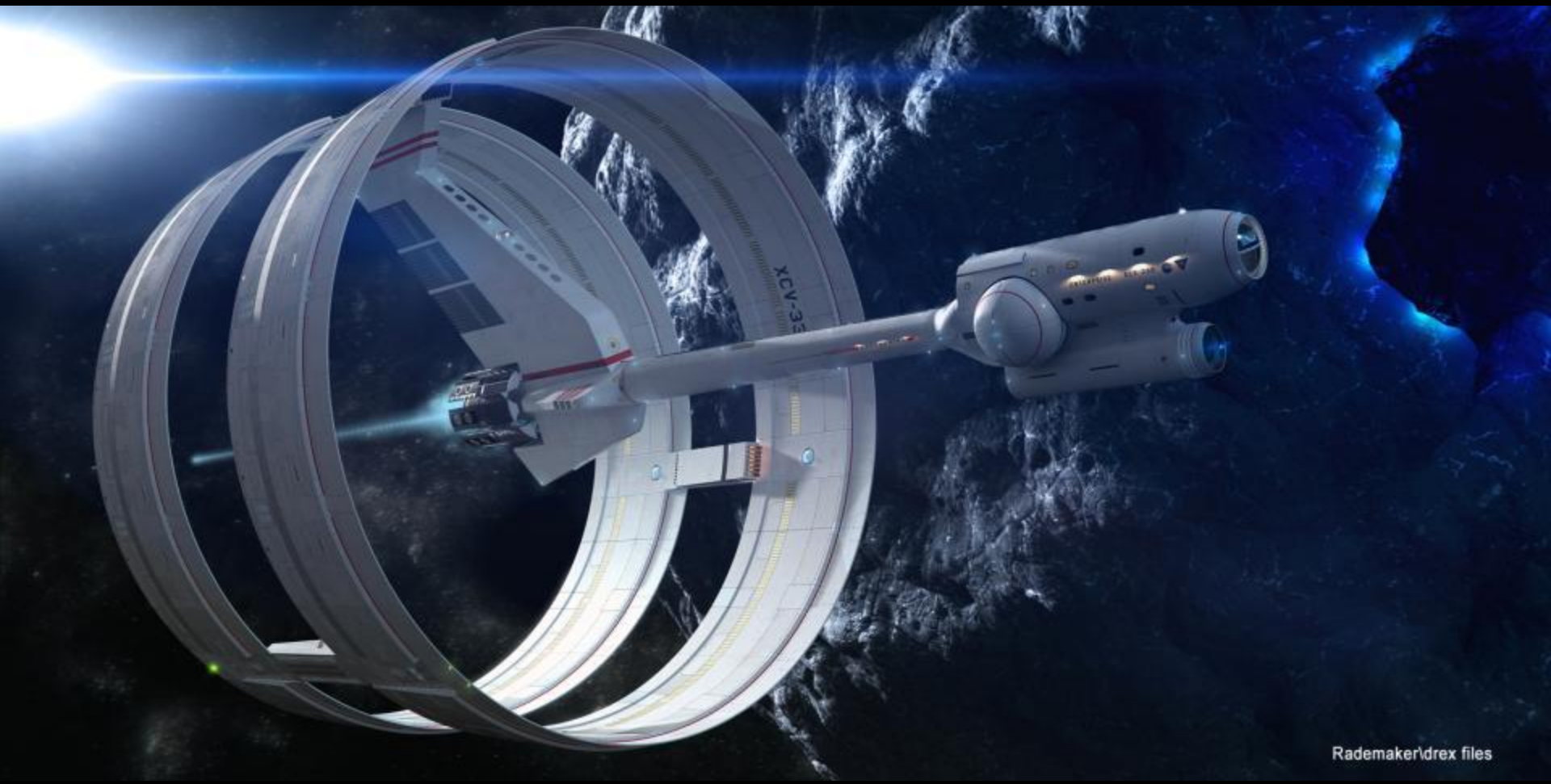

Matthew Jeffries is the artist that created the familiar Star Trek enterprise look

Updated concept based on Dr. White's theoretical findings, rendered by Mark Rademaker with artwork and inputs from Mike Okuda

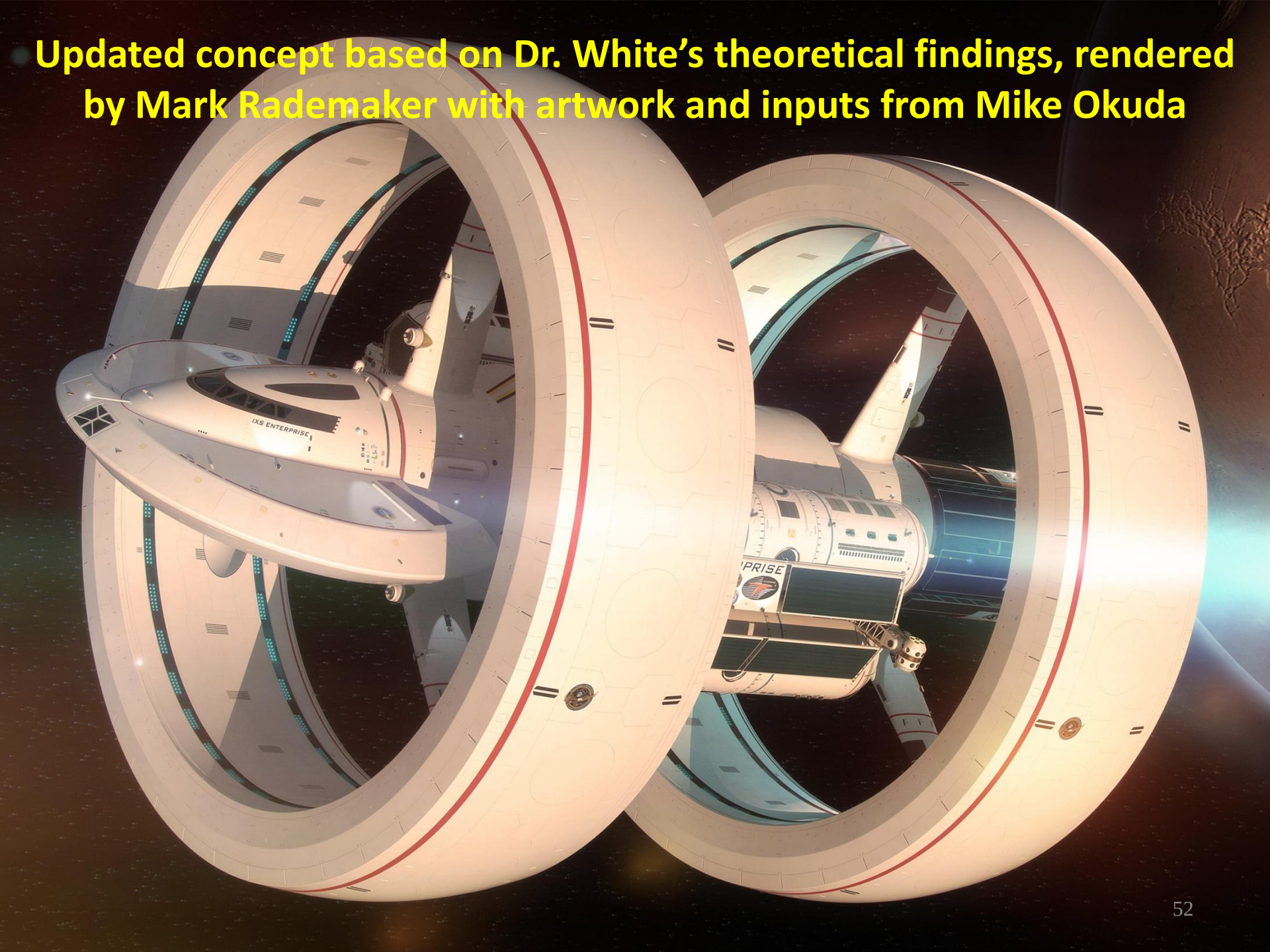

Updated concept based on Dr. White's theoretical findings, rendered by Mark Rademaker with artwork and inputs from Mike Okuda

EAGLEWORKS LABORATORIES

WARP FIELD PHYSICS VISION

ISS Deployable or Class D Mission

Reduced low thrust transit times (Reduced Alpha)

Fast Mars

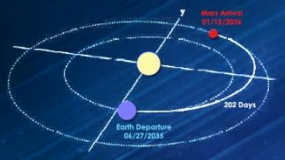

Reduced transit times for impulsive trajectories (Velocity Boost)

Fast Outer Solar System

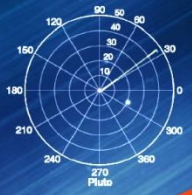

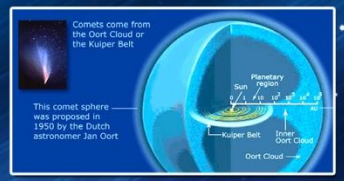

1,000 - 100,000 AU
- Interstellar Precursors

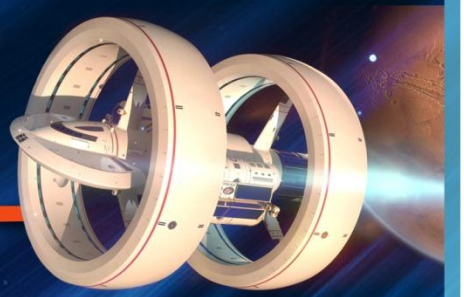

> 270,000 AU
Rapid Interstellar

1.5 - 50 AU

Aggregate negative pressure generators in desired topology to enable a progression of increasingly distant space mission destinations

0.1 AU

TERRESTRIAL PHASE

Drop Test
(Reduced drop time)

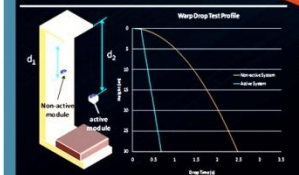

Ballistic Trajectories Evaluation
(Reduced parabola transit time)

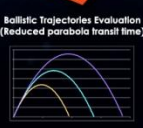

Time of Flight
(Reduced photon transit time)

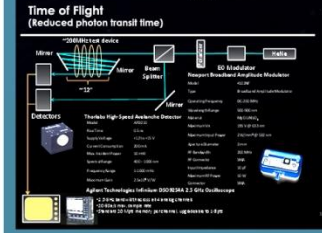

Warp Field Interferometer

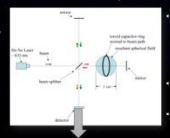

- Warp Field Interferometer developed after putting metric into canonical form[1].
- Generate microscopic warp bubble that perturbs optical index by 1 part in 10,000,000
- Induce relative phase shift between split beams that should be detectable.

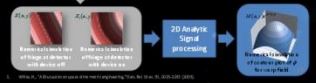

Interferometer
(Altered optics properties of space-time)

AU	POWER	#NPGs
>270k	Increasing Power	Increasing NPG Count
1k-100k		
1.5-50		
1.0-1.5		
0.1		

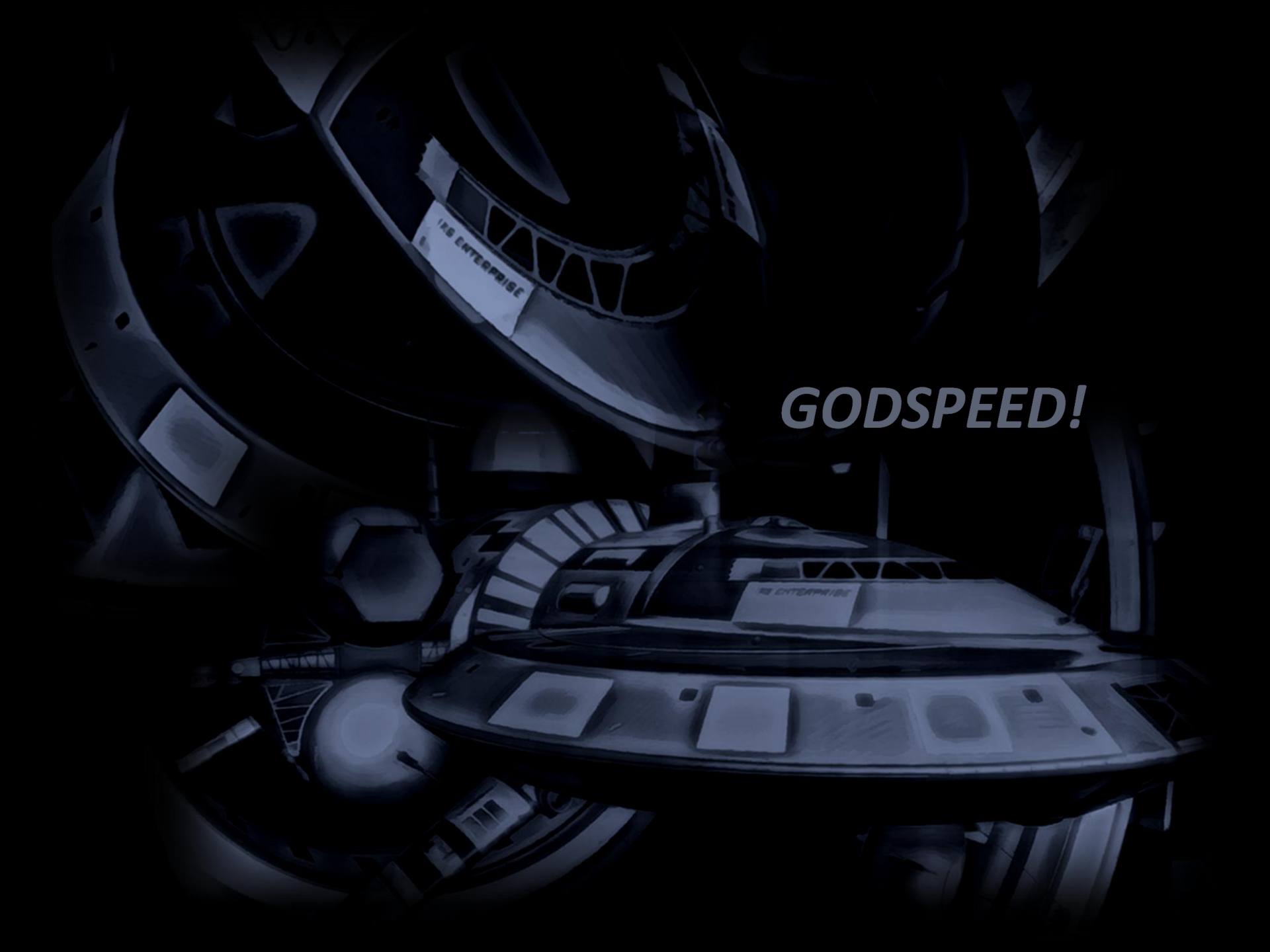
GODSPEED!

Principles of Q-thruster Operation

- Local mass concentrations, say in the form of a conventional capacitor with a ceramic dielectric, affect vacuum fluctuation density according to equation 1

$$\rho_{v_local} = \rho_v \sqrt{\frac{\rho_{m_local}}{\rho_v}} = \sqrt{\rho_{m_local}\rho_v} \qquad (1)$$

- Just as relativistic acceleration (Unruh radiation) can change the apparent relative density of the vacuum, so too can higher order derivatives according to equation 2.

$$\delta\rho = \frac{1}{4\pi G}\left(-\frac{1}{a^2}\left(\frac{da}{dt}\right)^2 + \frac{1}{a}\frac{d^2a}{dt^2}\right)$$

$$\delta\rho = \frac{1}{4\pi G}\left(\frac{1}{\phi^2}\left(\frac{d\phi}{dt}\right)^2 - \frac{1}{\phi}\frac{d^2\phi}{dt^2}\right) \qquad \vec{a} = -\nabla\phi \qquad (2)$$

- The tools of MagnetoHydroDynamics (MHD) can be used to model this modified vacuum fluctuation density analogous to how conventional forms of electric propulsion model propellant behavior.

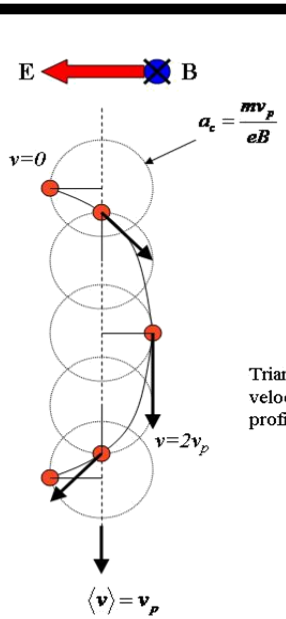

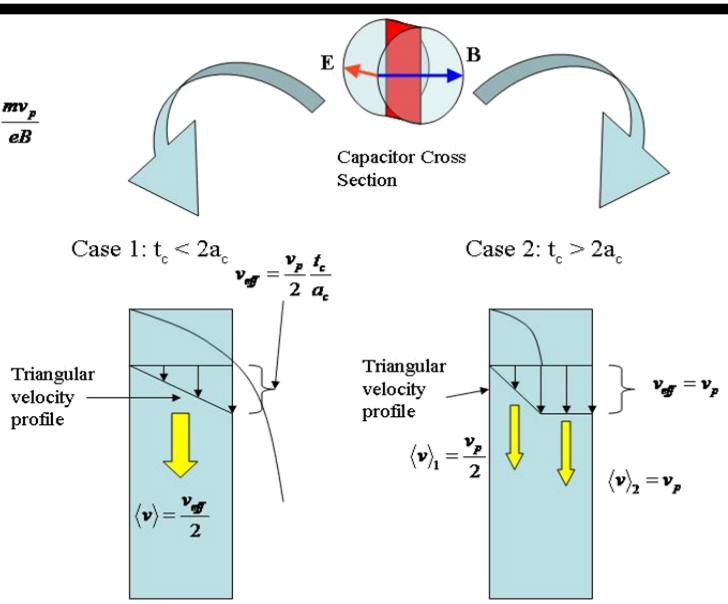

Gravitational Coupling Constant

- **Consider the following thought experiment: what would an inertial observer in deep space find if the dark energy density were to be integrated over the light horizon of the observable universe, ~13.7 billion light years?**
- **Starting with the Friedman Equation (and after some manipulation), the following equation can be derived that formally captures the results of this thought experiment:**

Vacuum Energy Density

$$\frac{2}{3}\rho_0 c^2 4\pi c^2 t_H{}^2 = \frac{c^4}{G}$$

Equation can be rearranged into the following form

$$G = \frac{1}{4\pi t_H{}^2 \frac{2}{3}\rho_0}$$

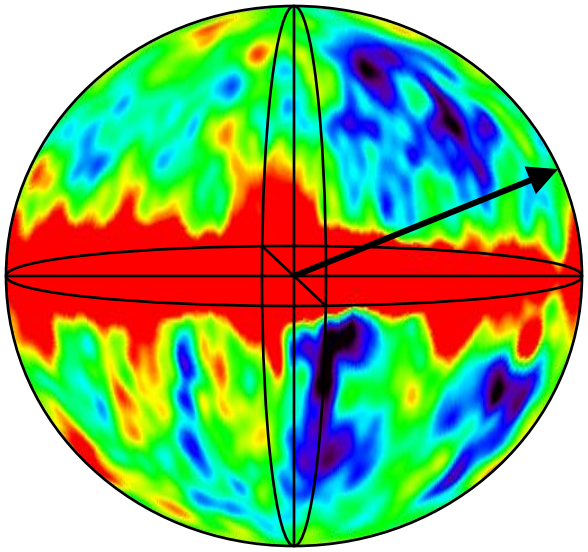

Light horizon

- **Using 9.9x10^{-27} kg/m^3 [2] with t_H of 13.7 billion years yields a predicted value for the gravitational constant of 6.45x10^{-11} m^3/kg·s^2**
- **A possible physical meaning to this rearranged equation solved for G is that gravitation is an emergent phenomenon rather than a fundamental force.**
- **To be specific, the claim could be made that the gravitational coupling constant may be a long wavelength consequence ($\lambda = ct_H$) of dark energy.**

Bohr Radius

- The vacuum perturbation equation just derived can be used to evaluate the state of the quantum vacuum in close proximity of the proton at the center of the Hydrogen atom.
- The first step is to calculate a quasi-classical density for the hydrogen nucleus. The radius of the hydrogen atom nucleus is given as R_0=1.2x10^{-15}m ($R=R_0 \cdot A^{1/3}$ where R_0 = 1.2x10^{-15}m and A is the atomic number - these are experimentally determined by electron scattering).
- The radius can be used with the mass of a proton to calculate a quasi-classical density of the hydrogen nucleus:

$$\rho_m = \frac{m_p}{\frac{4}{3}\pi R_0^{\,3}} = 2.31x10^{17}\ \frac{kg}{m^3}$$

- Using $\rho_v = {}^2/_3$ * 9.9x10^{-27} kg/m^3, along with this quasi-classical density ρ_m, the perturbed negative pressure state of the quantum vacuum around the hydrogen nucleus is calculated to be:

$$\rho_{v_local} = \sqrt{\rho_m \rho_v} = 3.90x10^{-5}\ \frac{kg}{m^3}$$

- The question can be asked how much volume of this perturbed state of the quantum vacuum is needed to have the equivalent energy value as the ground state of Hydrogen (13.6eV or 2.18x10^{-18} Nm)

$$r = \left(\frac{E}{\rho_{v_local} c^2 \frac{4}{3}\pi} \right)^{\frac{1}{3}} = a_0$$

- The calculated radius is r = 5.29x10^{-11} m, which is an exact match to the given value for the Bohr Radius, a_0 = 5.29x10^{-11} m.

Electron Mass

- **Frank Wilczek, Nobel laureate: "We have achieved a beautiful and profound understanding of the origin of most of the mass of ordinary matter, but not of all of it. The value of the electron mass, in particular, remains deeply mysterious…"**
- **Consider the energy state of the perturbed quantum vacuum field around the proton, and set this equal to the kinetic energy of the orbiting electron at the ground state.**

$$\frac{4}{3}\pi a_0{}^3 \rho_{v_local} c^2 = \frac{1}{2} m_e v^2$$

- **We know the speed of the orbiting electron:**

$$v = \alpha c = c/137$$

- **We can solve for the electron mass, and using the predicted value for ρ_{v_local} of 3.9x10^{-5} kg/m^3, we get a predicted electron mass of 9.1x10^{-31}kg.**

$$m_e = \frac{\frac{8}{3}\pi a_0{}^3 \rho_{v_local} c^2}{\left(\frac{c}{137}\right)^2}$$

Magnetic Pressure

- **The first step now is to calculate the magnetic pressure around the Hydrogen nucleus.**

The magnetic field as perceived by the electron is given by the following relationship. The speed of the orbiting electron is αc.

$$B = \frac{\mu_0 q v}{4\pi a_0^{\,2}}$$

The magnetic pressure is a simple calculation:

$$\frac{B^2}{2\mu_0} = 6.25x10^7 \ {}^{N}\!/_{m^2}$$

- **The quasi-classical plasma pressure of the perturbed quantum vacuum state around the Hydrogen nucleus can be calculated by converting the electron velocity to temperature using 1/2 $m_e v^2 = kT$, and making the assumption that the virtual electron-positron plasma has the same effective temperature as the orbiting electron.**
- **When the plasma pressure calculation makes use of a 2/3 factor, analogous to the predicted dark energy fraction of 2/3 picked up during integration to calculate the Gravitational constant, the values are nearly identical:**

$$P = n_e kT = \frac{2}{3}\frac{\rho_{v_local}}{m_e} kT = 6.24x10^7 \ {}^{N}\!/_{m^2}$$